

Intersection of nuclear structure and high-energy nuclear collisions 2026

Imaging nuclear structure across energy scales: from heavy to light ions

Chunjian Zhang

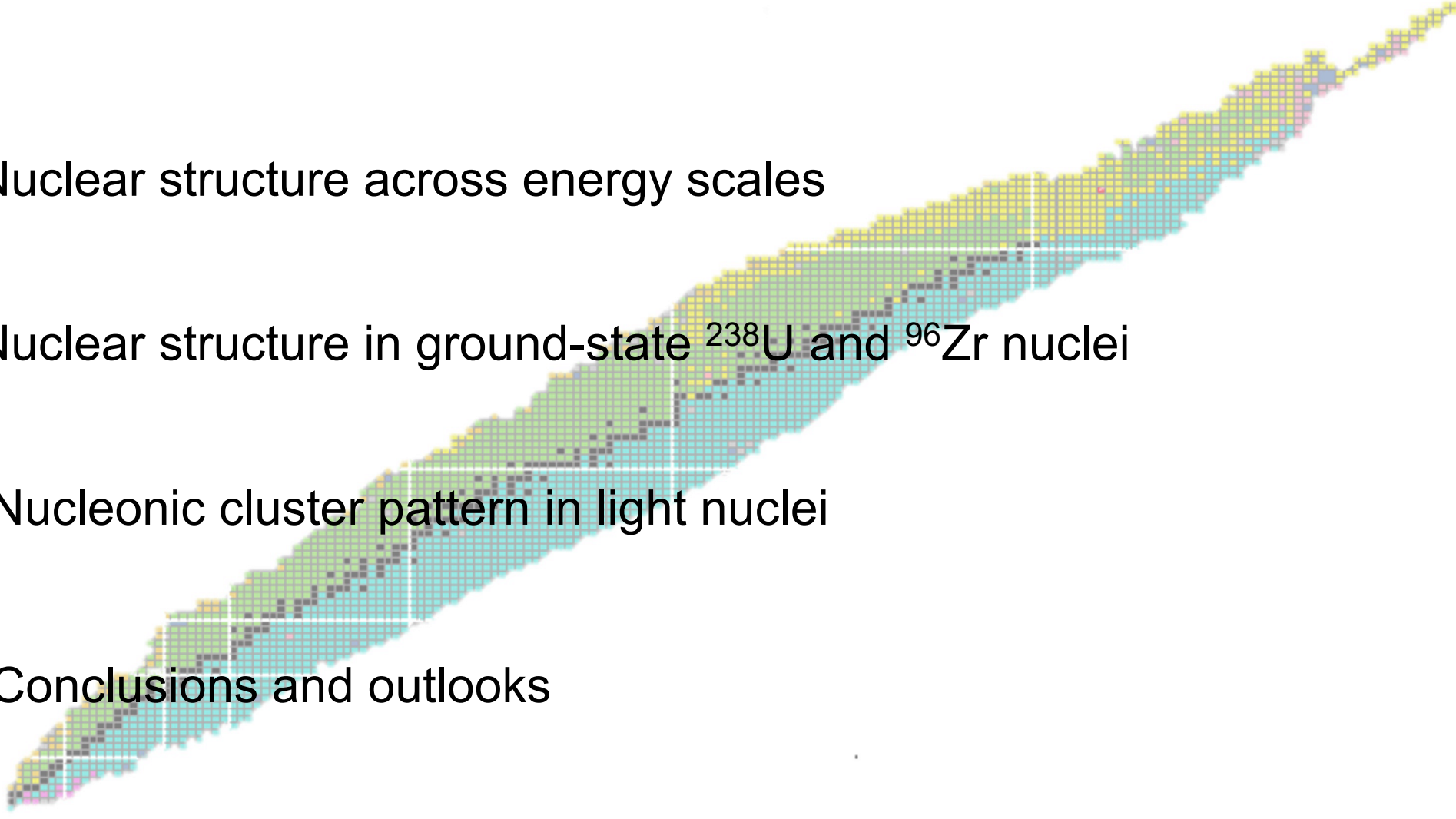
Fudan University

April 13-24, 2026

Yukawa Institute for Theoretical Physics

Kyoto University

Outline

- 
- I. Nuclear structure across energy scales
 - II. Nuclear structure in ground-state ^{238}U and ^{96}Zr nuclei
 - III. Nucleonic cluster pattern in light nuclei
 - IV. Conclusions and outlooks

Collective structure of atomic nuclei

- Emergent phenomena of the many-body quantum system

- Non-monotonic evolution with N and Z
- Quadrupole/octupole/hexadecapole deformations
- Clustering, halo, skin, bubble...

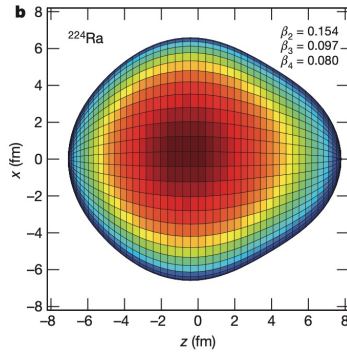
Y. Ye, X. Yang, H. Sakurai, B. Hu, *Nature Review Physics*, 7, 21-37 (2025)

Y.-G. Ma, S. Zhang, *Handbook of Nuclear Physics* (2022)

Quadrupole



Octupole

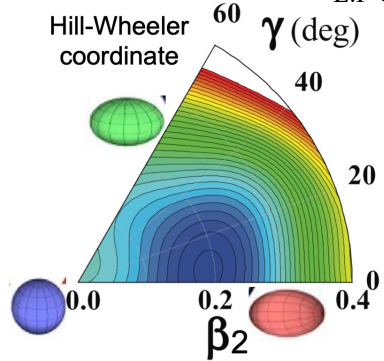


S. Cwiok et al., *Nature* 433, 705 (2005)

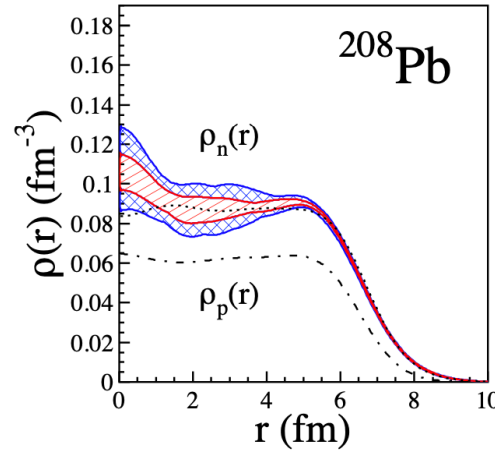
L.P Gaffney et al., *Nature* 497, 199 (2013)

Hill-Wheeler coordinate

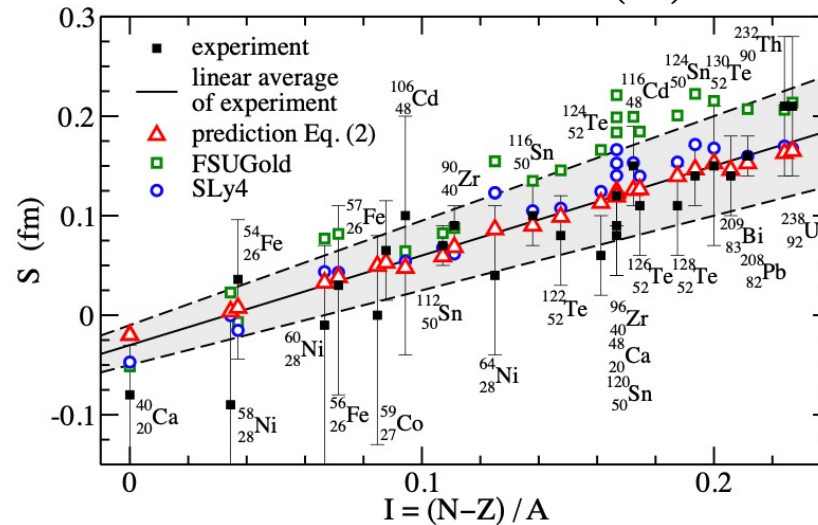
Triaxial spheroid



A. Andreyev et al., *Nature* 405, 430 (2000)



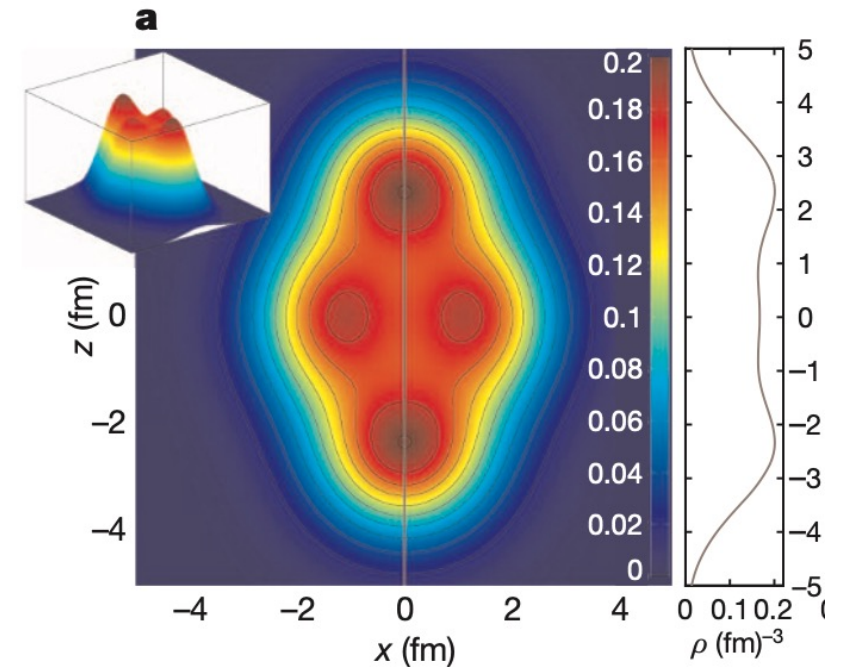
Neutron skin



A. Trzcinska et al., *PRL* 87, 082501 (2001)

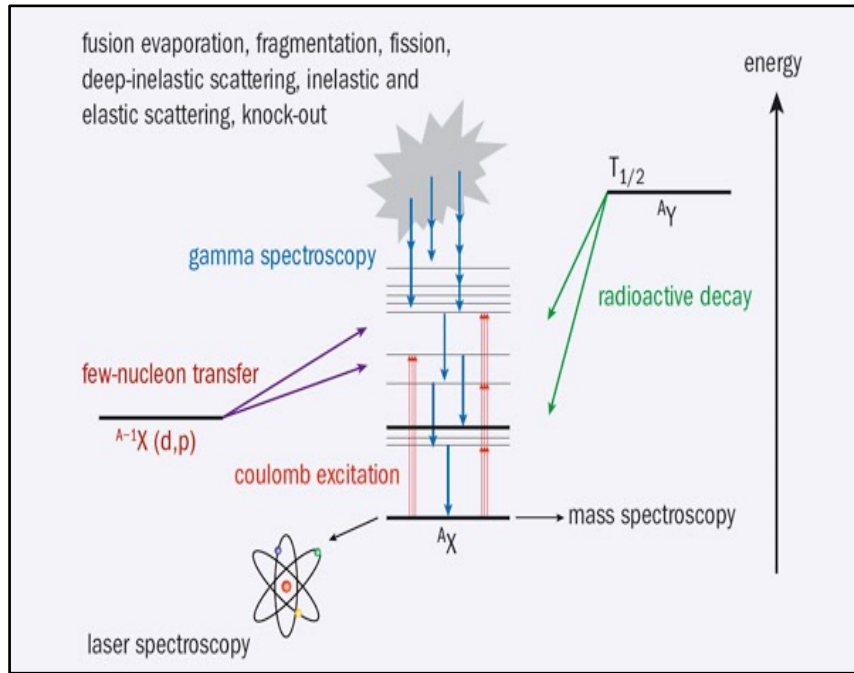
A. M. Centelles et al., *PRL* 102, 122502 (2009)

nucleonic clustering

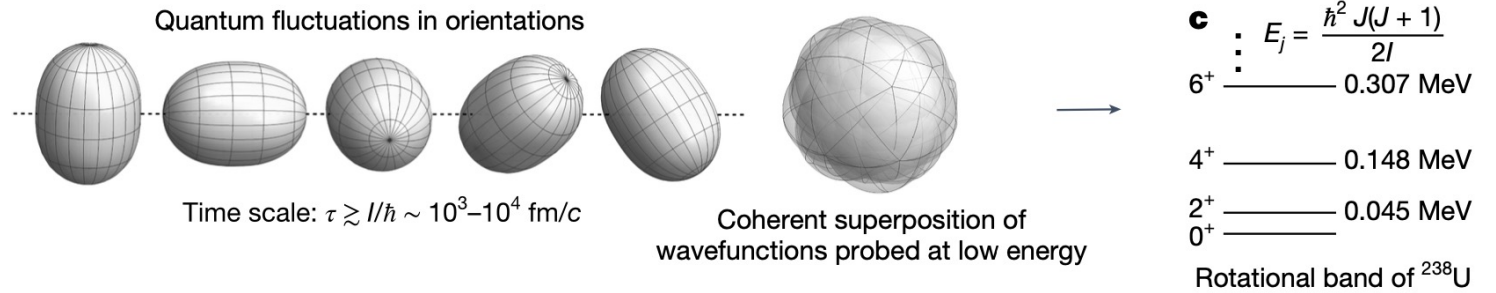


J.P. Ebran et al., *Nature* 487, 341 (2012)

Nuclear shape at low energy: long exposure

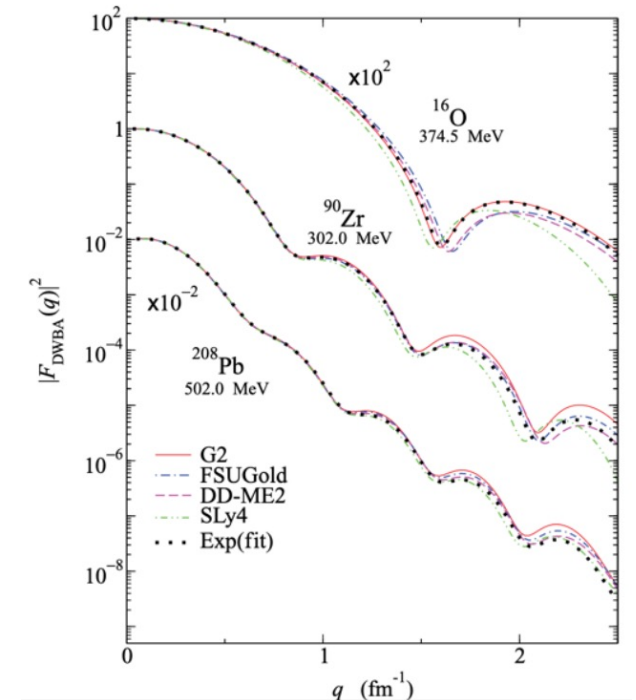
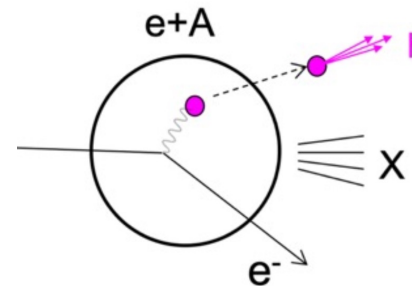


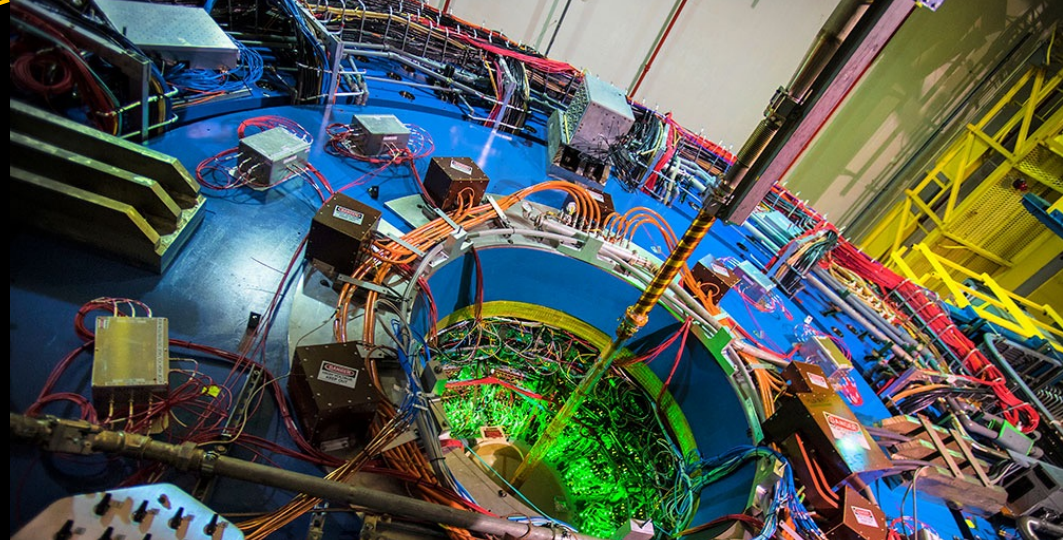
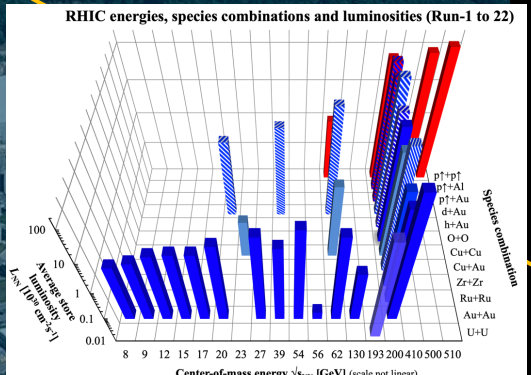
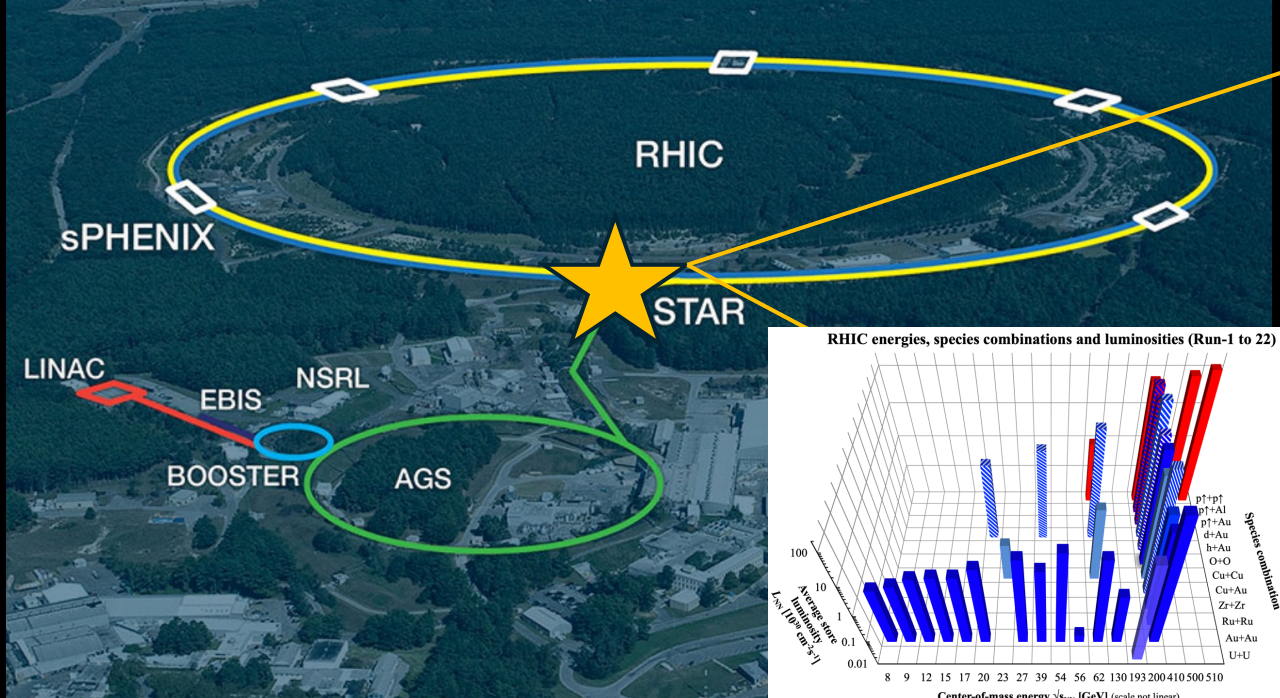
Each DOF has zero-point fluctuations within an intrinsic timescale.



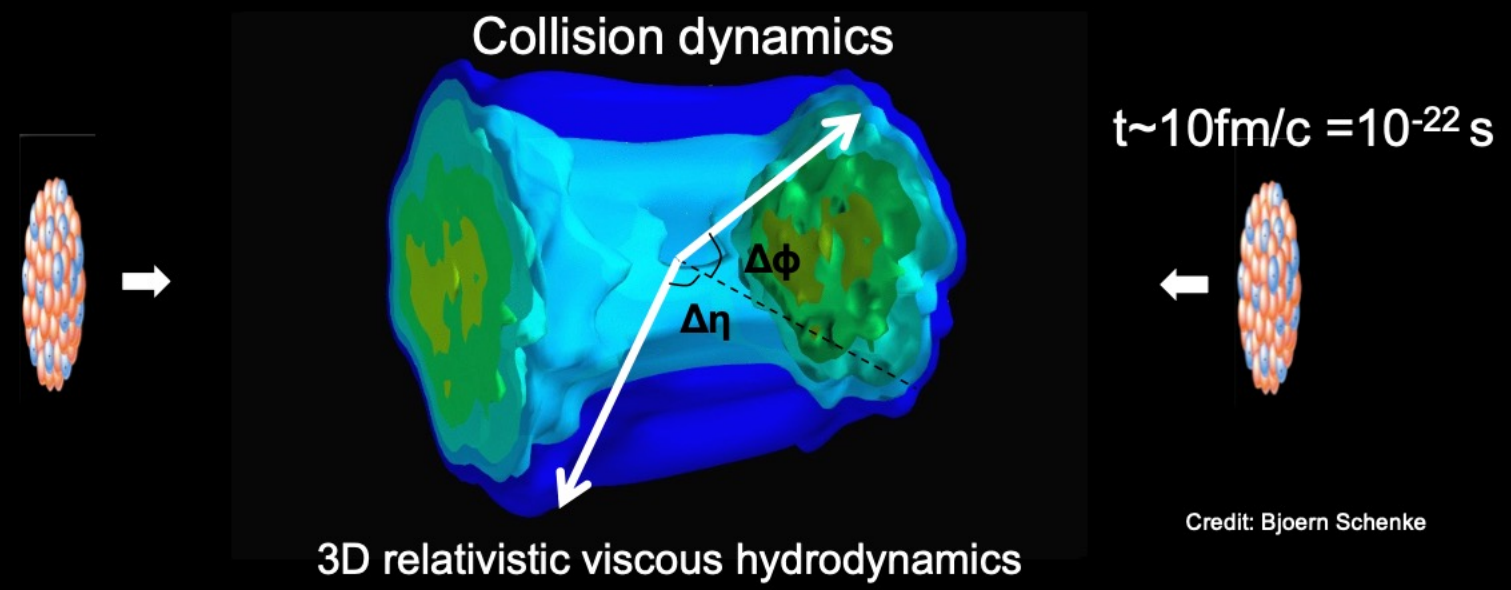
probe a superposition of these fluctuations, instantaneous shapes not directly seen

$e+A$ scattering has very short timescales, but so far mostly imaged the one-body (charge) distribution. The impact of deformation appears as an increase in the radius





- 1) large, uniform acceptance at mid-rapidity
- 2) A vast number of emitted final state hadrons
- 3) capability to access nuclear structures in different collisions...



Imaging by smashing method

Take a snapshot

Evolution

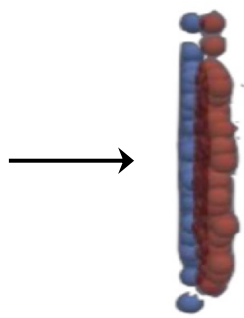
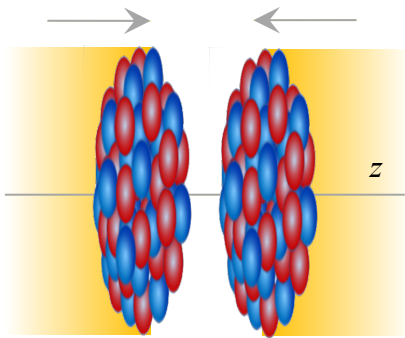
Measurement

Nuclei collisions

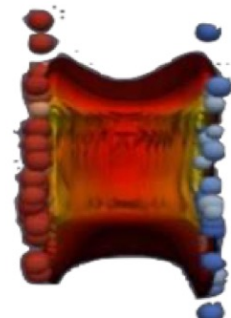
$$T_{\mu\nu}(\tau = 0)$$

$$\partial_\mu T^{\mu\nu} = 0, \text{ EOS, viscosity...}$$

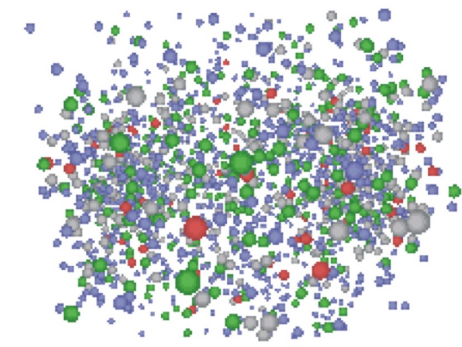
$$T_{\mu\nu}(\tau = \infty)$$



Pressure-driven expansion of
Quark-gluon plasma (QGP)



free-streaming



$\tau \sim 2R_0/\Gamma \sim 0.1 \text{ fm}/c$
exposure

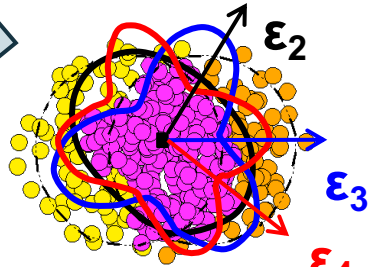
$\tau \sim 10 \text{ fm}/c$
expansion

$\tau \sim 10^{15} \text{ fm}/c$
detection

$$\rho(r, \theta, \phi) = \frac{\rho_0}{1 + e^{(r-R(\theta, \phi))/a_0}}$$

- $\beta_2 \rightarrow$ quadrupole deformation
- $\beta_3 \rightarrow$ octupole deformation
- $\gamma \rightarrow$ triaxiality
- $a_0 \rightarrow$ surface diffuseness
- $R_0 \rightarrow$ nuclear size

ab initio theory/shell model/DFT



size & shape

J. Jia et al., *Nucl. Sci. Tech.* 35, 220 (2024)

$$R_\perp^2 \propto \langle r_\perp^2 \rangle \quad \mathcal{E}_n \propto \langle r_\perp^n e^{in\phi} \rangle$$

Diagram showing the relationship between R_0 , a_0 , and β_n and the deformation parameters \mathcal{E}_n .

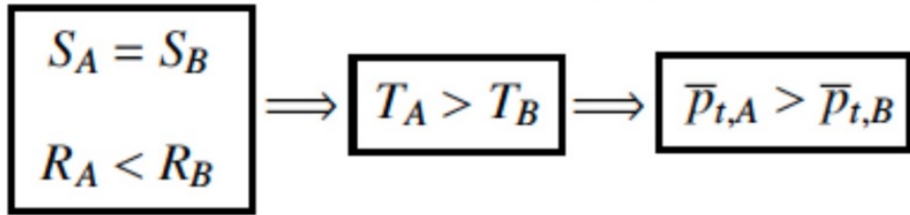
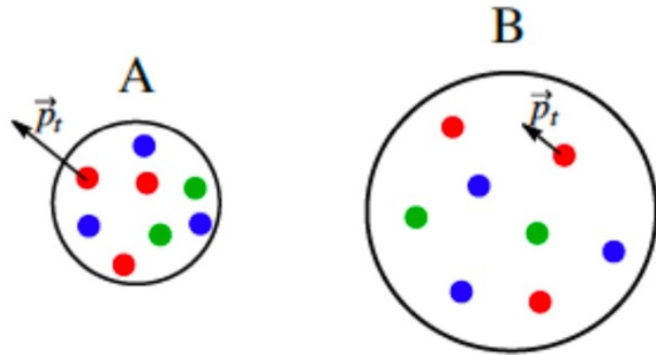
Observables $\frac{d^2 N}{d\phi dp_T} = N(p_T) \left(\sum_n V_n e^{-in\phi} \right)$

Event-by-event linear responses:

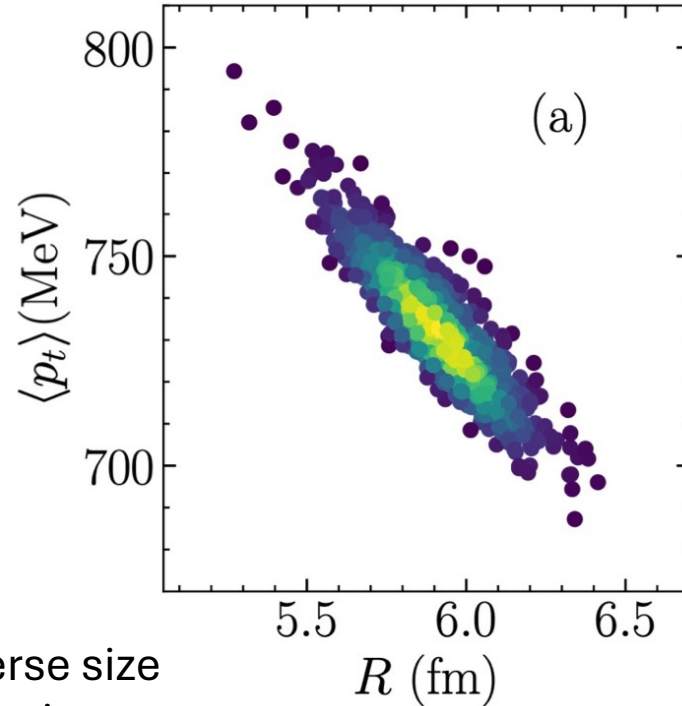
$$\frac{\delta[p_T]}{[p_T]} \propto -\frac{\delta R_\perp}{R_\perp} \quad V_n \propto \mathcal{E}_n$$

Key: 1) fast snapshot, 2) linear response, 3) large multiplicity for many-body correlation

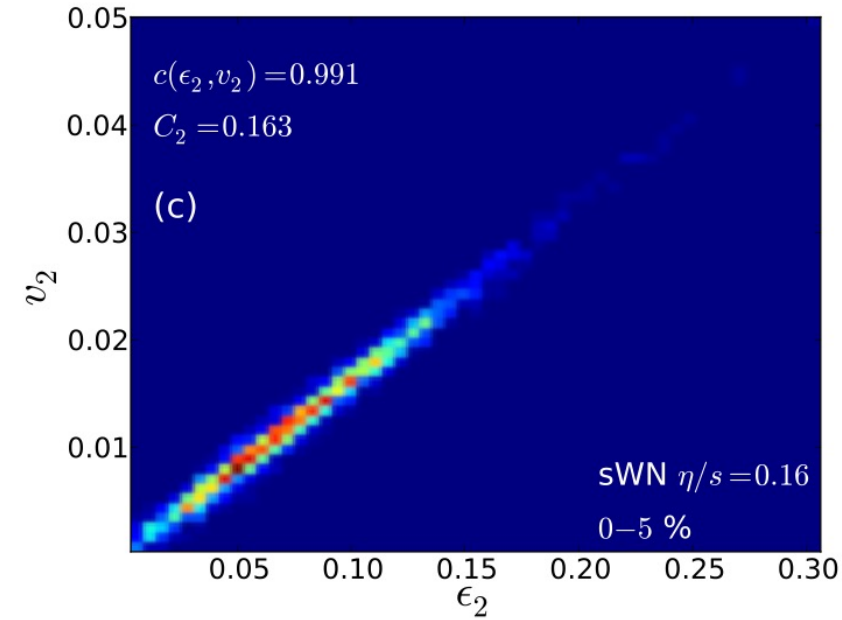
Linear response in ultra-central collisions



G. Giacalone et al., *PRC* 103, 024909 (2021)



H. Niemi et al., *PRC* 87, 054901 (2013)



Same total energy deposition, **smaller** transverse size in the initial state creates **stronger** radial expansion.

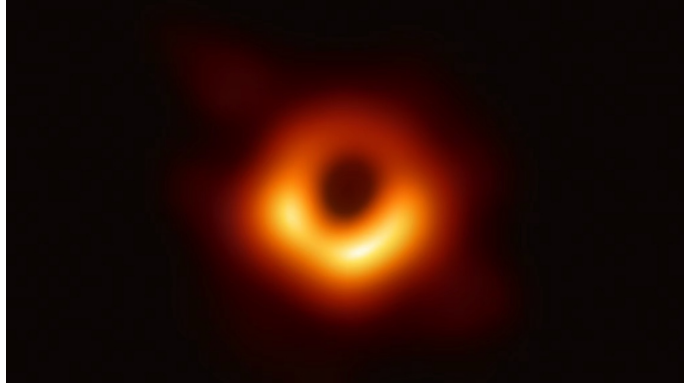
$$\delta[p_T] \propto -\delta R \propto \delta d_{\perp}$$

$$v_n \propto \epsilon_n$$

Linear relations permit us to image colliding nuclear shapes.

Analogy to the snapshot imaging technique

First-ever image of a black hole



MRI CT image

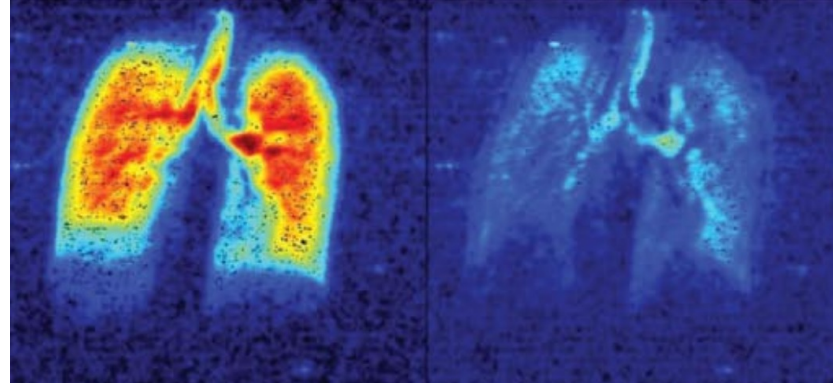
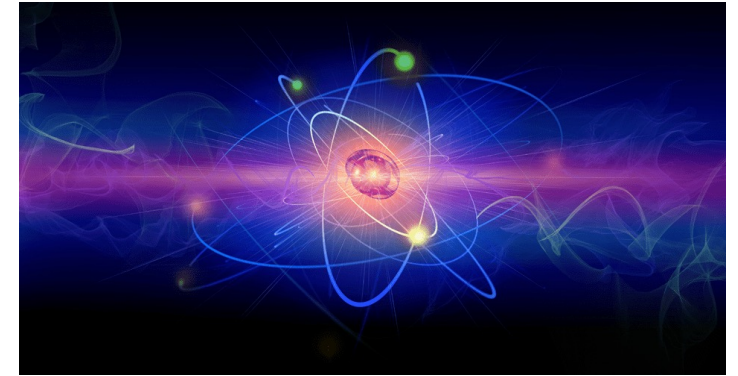


Image of electrons at attosecond



Astronomical scale

Microscopic scale

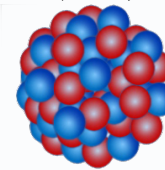
J. Jia et al., *Nucl. Sci. Tech.* 35, 220 (2024), G. Giacalone, *EPJA* 59, 297 (2023), T. Duguet et al., *PRL* 135, 182301 (2025) W. Ke, 2509.09549, ...

Emergent seeing shape directly require access to instantaneous nucleon distributions

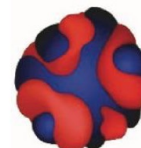
Will see all DOFs longer than exposure timescale:

nucleons, hadrons, quark, gluons, gluon saturations

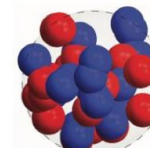
$$\Psi(\mathbf{r}_1, \mathbf{r}_2, \dots)$$



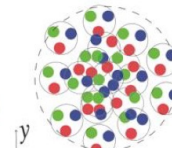
$\ll 1$ MeV



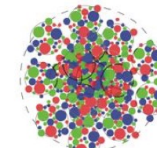
$\sim 1-10$ MeV



~ 100 MeV



~ 1 GeV



$\gtrsim 100$ GeV

$\rightarrow \sqrt{s_{NN}}$

Yoctosecond scale

$$\begin{aligned} 1\text{fm}/c &= 3 \times 10^{-24} \text{ seconds} \\ &= 3 \times 10^{-6} \text{ attoseconds} \\ &= 3 \text{ yoctoseconds} \end{aligned}$$

A new, complementary, and independent of low-energy experiments

Analogy to the snapshot imaging technique

Eileen Gu@2022



Short-time-scale imaging could reveal detailed shapes.

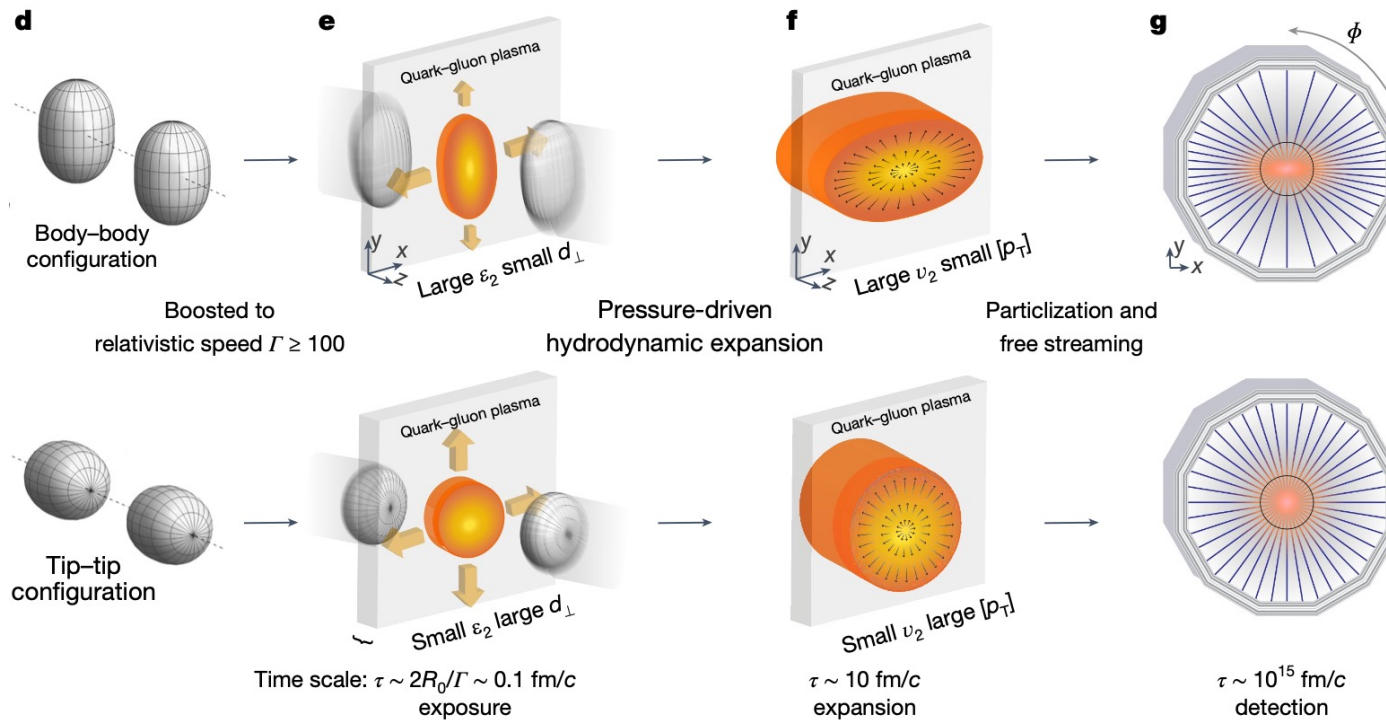
Imaging nuclear shape in high-energy snapshot

- Nuclear shape in intrinsic (body-fixed) frame not directly visible in the lab frame
 - Mainly inferred from non-invasive spectroscopy methods.

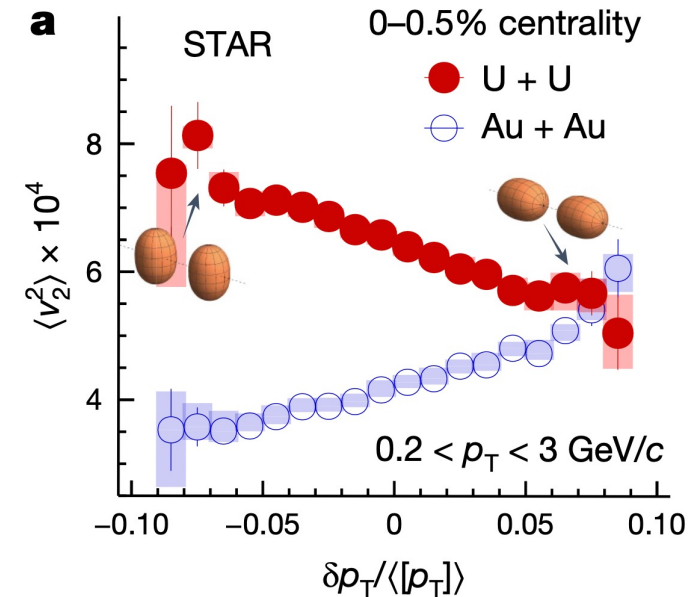
Nuclear deformation across energy scales

STAR, *Nature* 635, 67-72 (2024)

Nature News&Views, News, Podcast



Body-body: $v_2 \nearrow p_T \searrow$



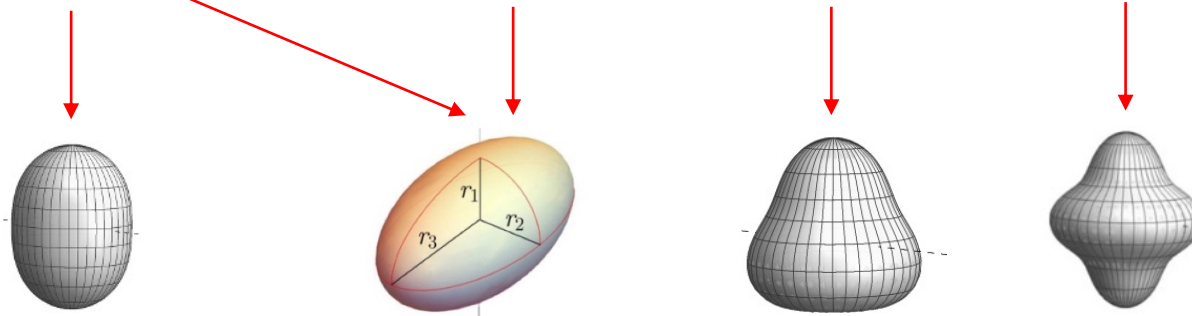
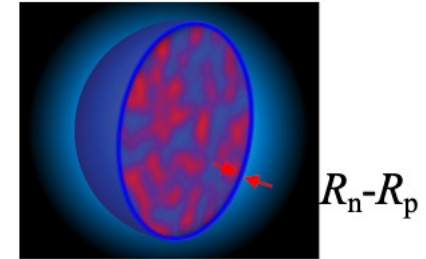
Tip-tip: $v_2 \searrow p_T \nearrow$

Shape-frozen like a snapshot during nuclear crossing (10^{-25} s \ll rotational time scale 10^{-21} s)
 probe entire mass distribution in the intrinsic frame via multi-point correlations

II. Nuclear structure in ground-state ^{238}U and ^{96}Zr nuclei

$$\rho(r, \theta, \phi) = \frac{\rho_0}{1 + e^{(r-R(\theta,\phi))/a_0}}$$

$$R(\theta, \phi) = R_0 (1 + \beta_2 [\cos \gamma Y_{2,0}(\theta, \phi) + \sin \gamma Y_{2,2}(\theta, \phi)] + \beta_3 Y_{3,0}(\theta, \phi) + \beta_4 Y_{4,0}(\theta, \phi))$$



W. Ryssens, G. Giacalone, B. Schenke, C. Shen, *PRL* 130, 212302 (2023)

DFT calculations predict a slightly small WS deformation

$$\beta_{2\text{U}} \approx 0.28 \rightarrow \beta_{2\text{U,WS}} \approx 0.25$$

corresponding to a larger volume deformation in presence of $\beta_{4\text{U}} \sim 0.1$ $\beta_{2,\text{body}} = \frac{4\pi}{3R_0^2 A} \int d^3r \rho(\mathbf{r}) r^2 Y_{20}$

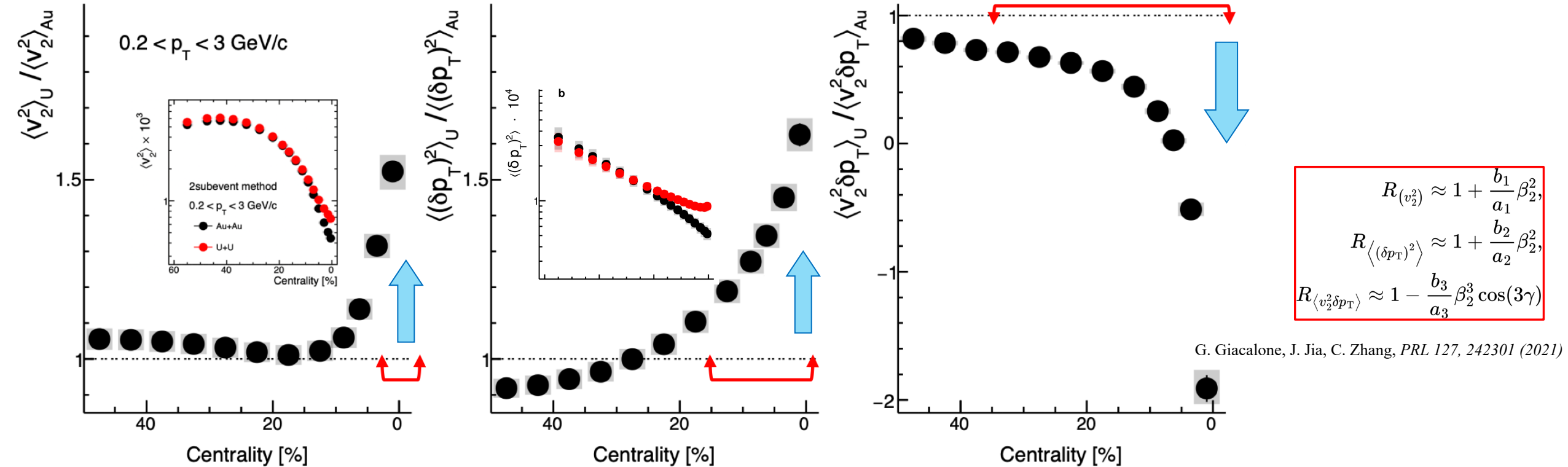
Low-energy estimate with rigid rotor assumption from B(E2) data $\beta_{2,\text{LD}} = \frac{4\pi}{5R_0^2 Z} \sqrt{\frac{B(\text{E2})}{e^2}}$

$$\beta_{2\text{U,LD}} = 0.287 \pm 0.007 \quad \gamma_{\text{U,LD}} = 6^\circ - 8^\circ$$

$$\beta_{3\text{U}} \sim \beta_{4\text{U}} \sim 0.1$$

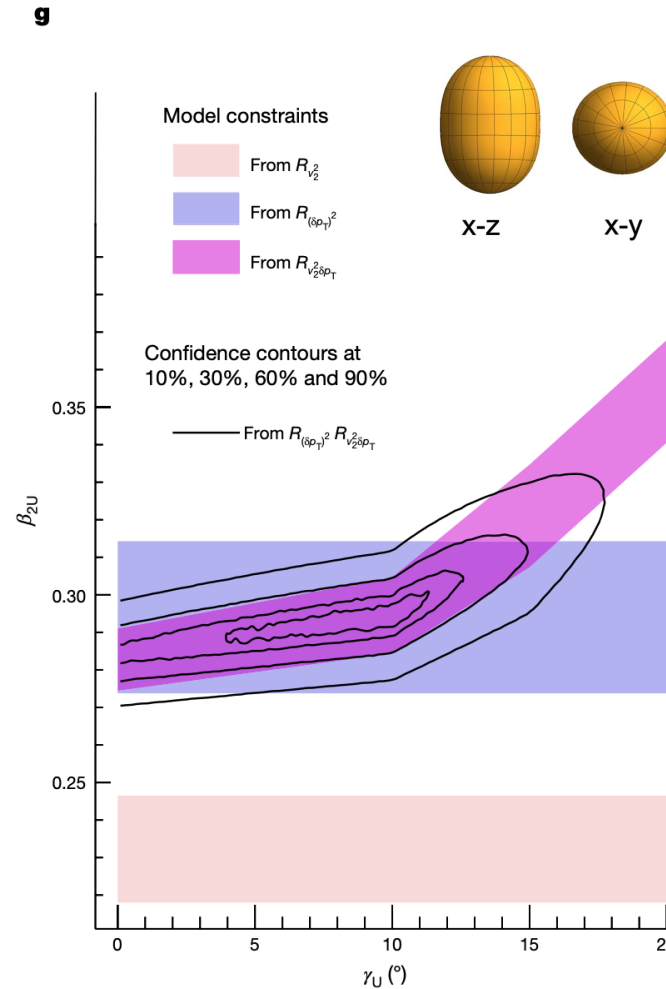
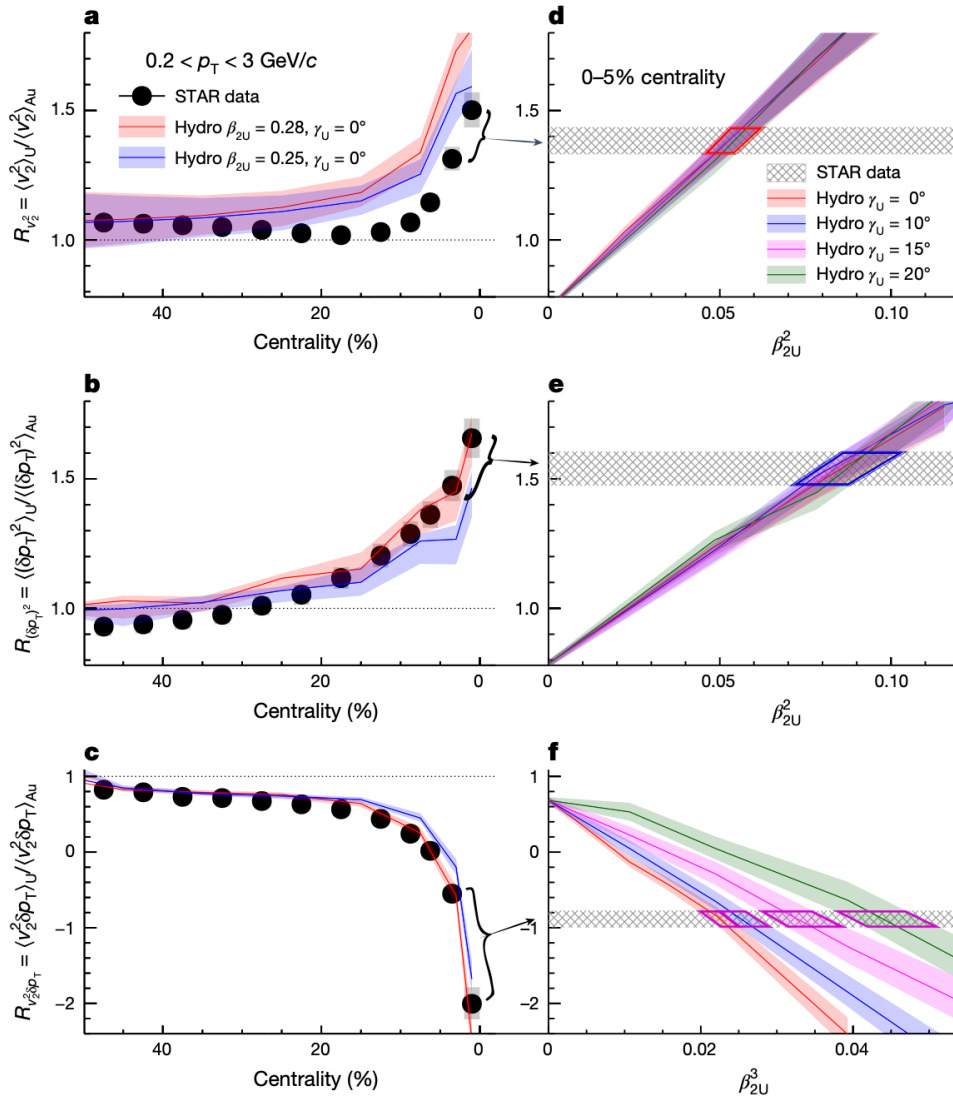
B. Pritychenko et al., *JADT*.107, 1 (2016)
C. Y. Wu et al., *PRC* 54, 2356(1996)

Ratio of observables



- Elliptic flow and size fluctuation are enhanced by the nuclear deformation effect.
- Ratios cancel final state effects and isolate the effects of initial state/nuclear structures.
→ U deformation dominates the ultra-central collisions (UCC)

Constraining the ground-state ^{238}U : $\beta_{2,U}$ and γ_U



Sufficient precision is achieved from ratios in ultra-central collisions
 Relation also confirmed from hydro

$$R_{(v_2^2)} \approx 1 + \frac{b_1}{a_1} \beta_2^2,$$

$$R_{\langle (\delta p_T)^2 \rangle} \approx 1 + \frac{b_2}{a_2} \beta_2^2,$$

$$R_{\langle v_2^2 \delta p_T \rangle} \approx 1 - \frac{b_3}{a_3} \beta_2^3 \cos(3\gamma)$$

High-energy estimate
 (*IP-Glasma+MUSIC and Trajectum*)

$\beta_{2U} = 0.286 \pm 0.025$

$\gamma_U = 8.5^\circ \pm 4.8^\circ$

low-energy estimate:

$\beta_{2U} = 0.287 \pm 0.007$

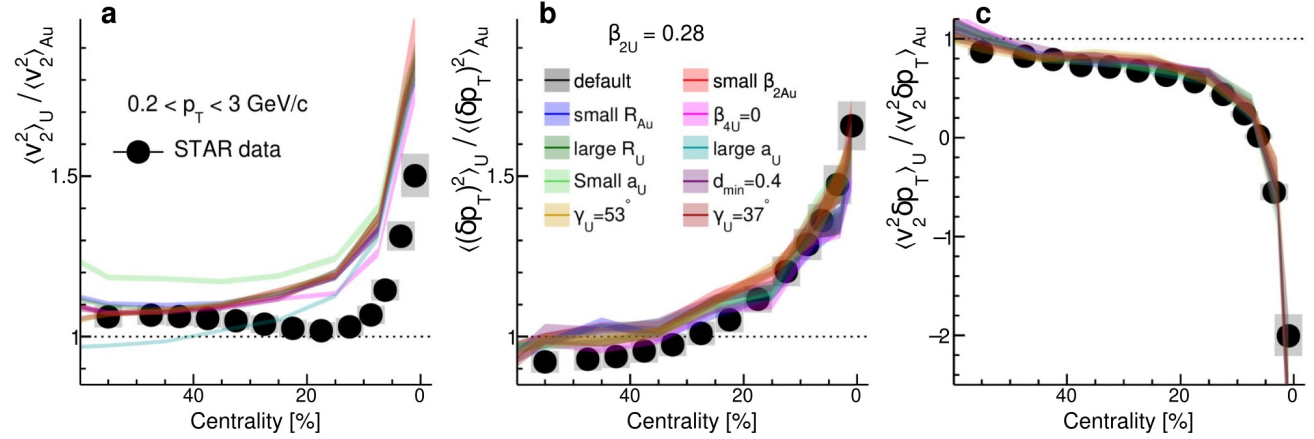
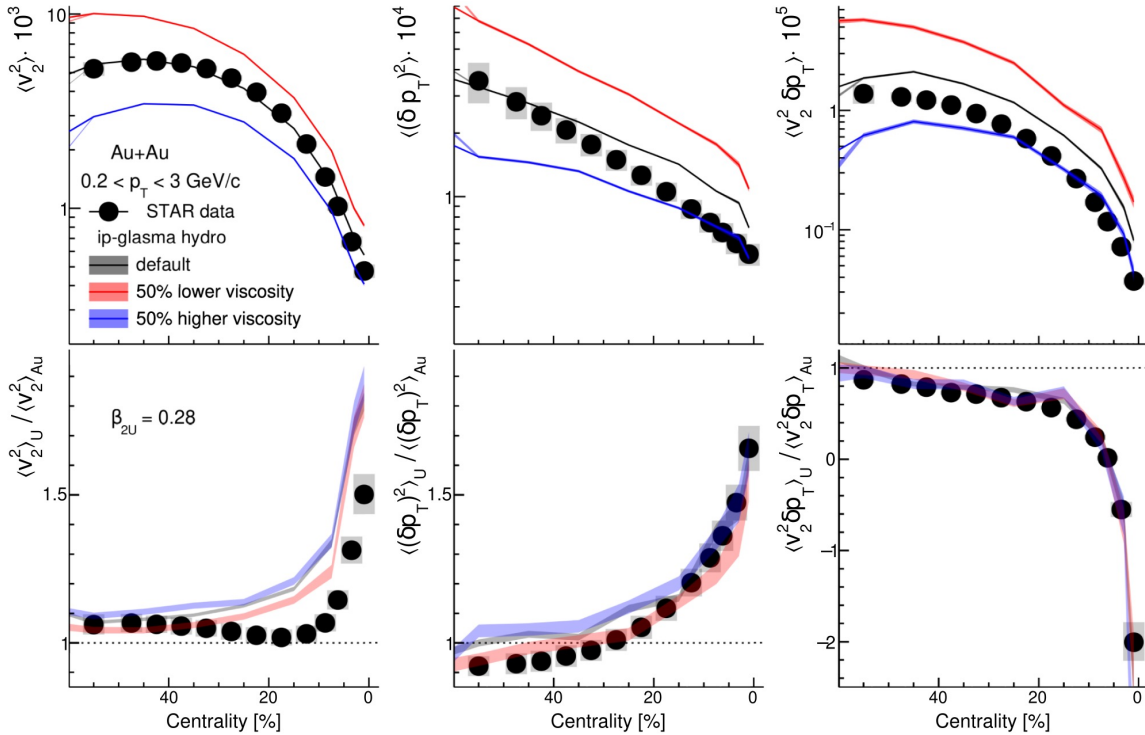
$\gamma_U = 6^\circ - 8^\circ$

A large deformation with a slight deviation from axial symmetry in the nuclear ground-state

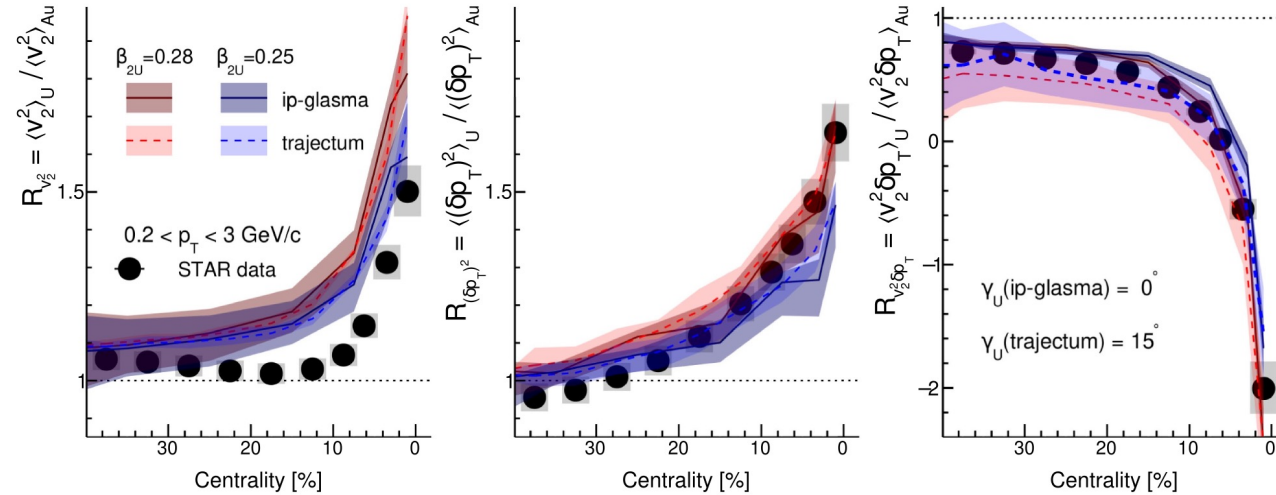
Viscosity, nuclear parameters, and model variations

2) Effect from nuclear parameters are small, included as model systematics.

1) Taking the ratios cancels the viscosity effects.



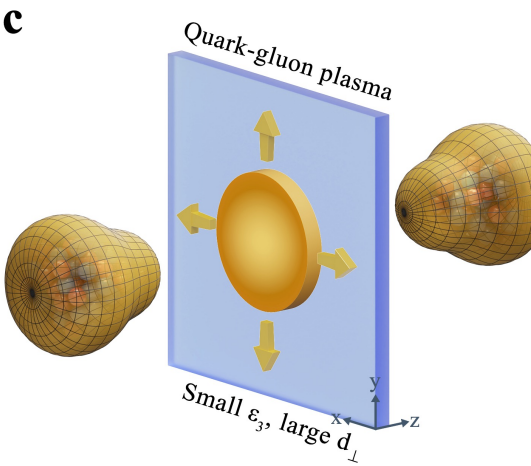
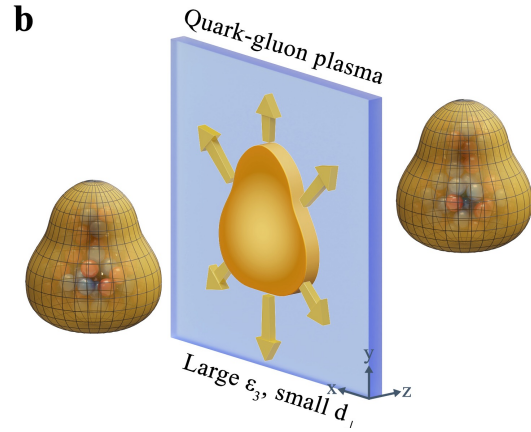
3) Another hydrodynamics model, Trajectum, shows rather consistent extractions even if it was not tuned to RHIC data.



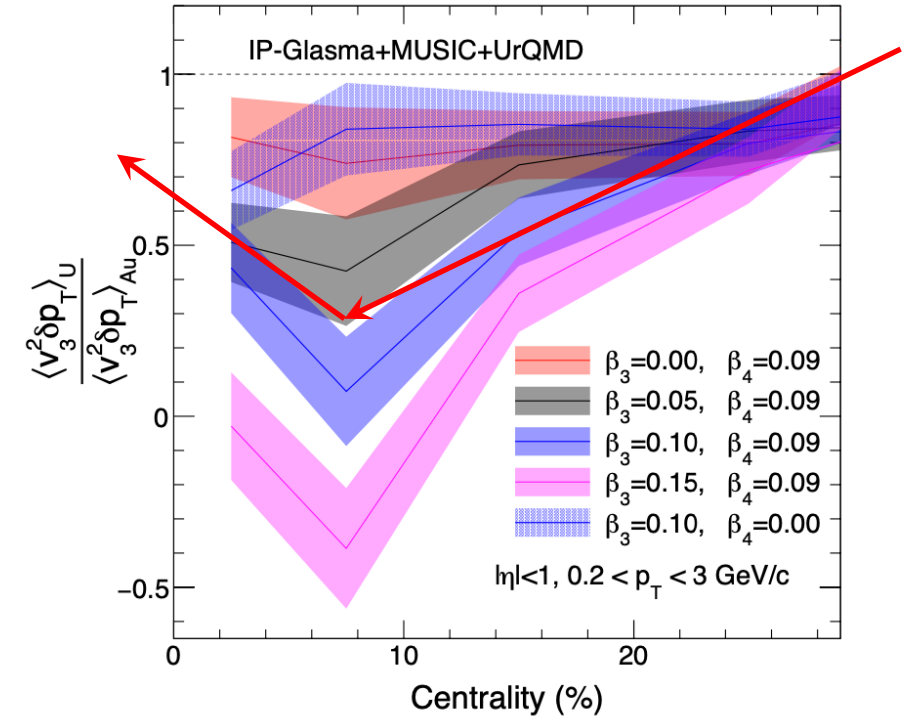
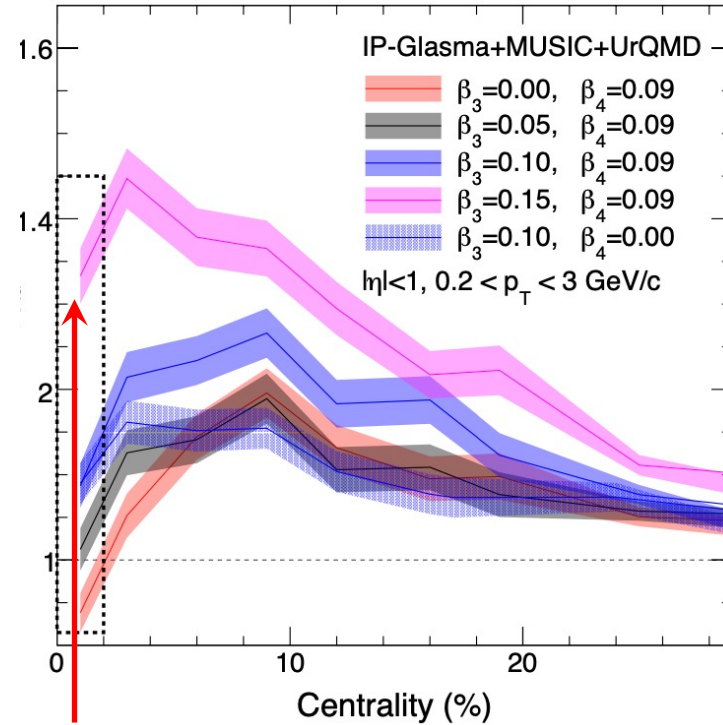
Extracted $\beta_{2,U}$ and γ_U values are robust.

Evidence of octupole deformation $\beta_{3,U}$

C. Zhang, J. Jia, J. Chen, C. Shen, L. Liu, 2504.15245



IP-Glasma+MUSIC calculations



However, v_3 is fluctuation driven, expect in central

$$\langle v_3^2 \rangle \propto \langle \varepsilon_3^2 \rangle \sim 1/A$$

mass number \nearrow

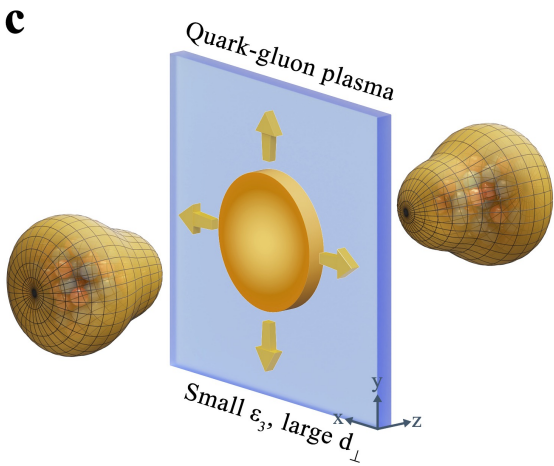
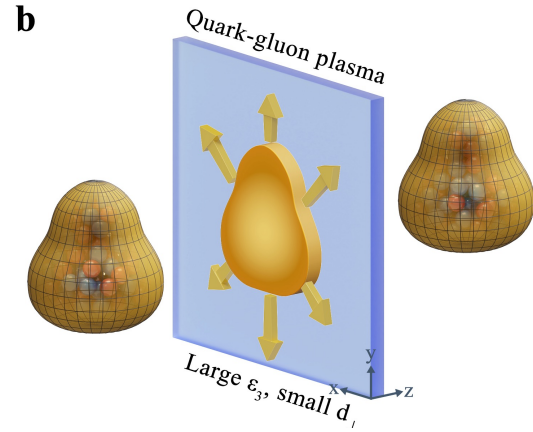
$\langle v_3^2 \rangle$ follows a linear increase with β_3^2 ,

Characteristic anticorrelation in $\langle v_3^2 \delta p_T \rangle$ shows a pronounced β_3 -dependent suppression.

$$R_{v_3^2} = \frac{\langle v_3^2 \rangle_{U+U}}{\langle v_3^2 \rangle_{Au+Au}} \approx \frac{a_{3U}}{a_{3Au}} + \frac{b_{3,3}}{a_{3Au}} \beta_3^2 + \frac{b_{3,4}}{a_{3Au}} \beta_4^2,$$

$$R_{v_3^2 \delta p_T} = \frac{\langle v_3^2 \delta p_T \rangle_{U+U}}{\langle v_3^2 \delta p_T \rangle_{Au+Au}} \approx a - b \beta_2 \beta_3^2.$$

Evidence of octupole deformation $\beta_{3,U}$

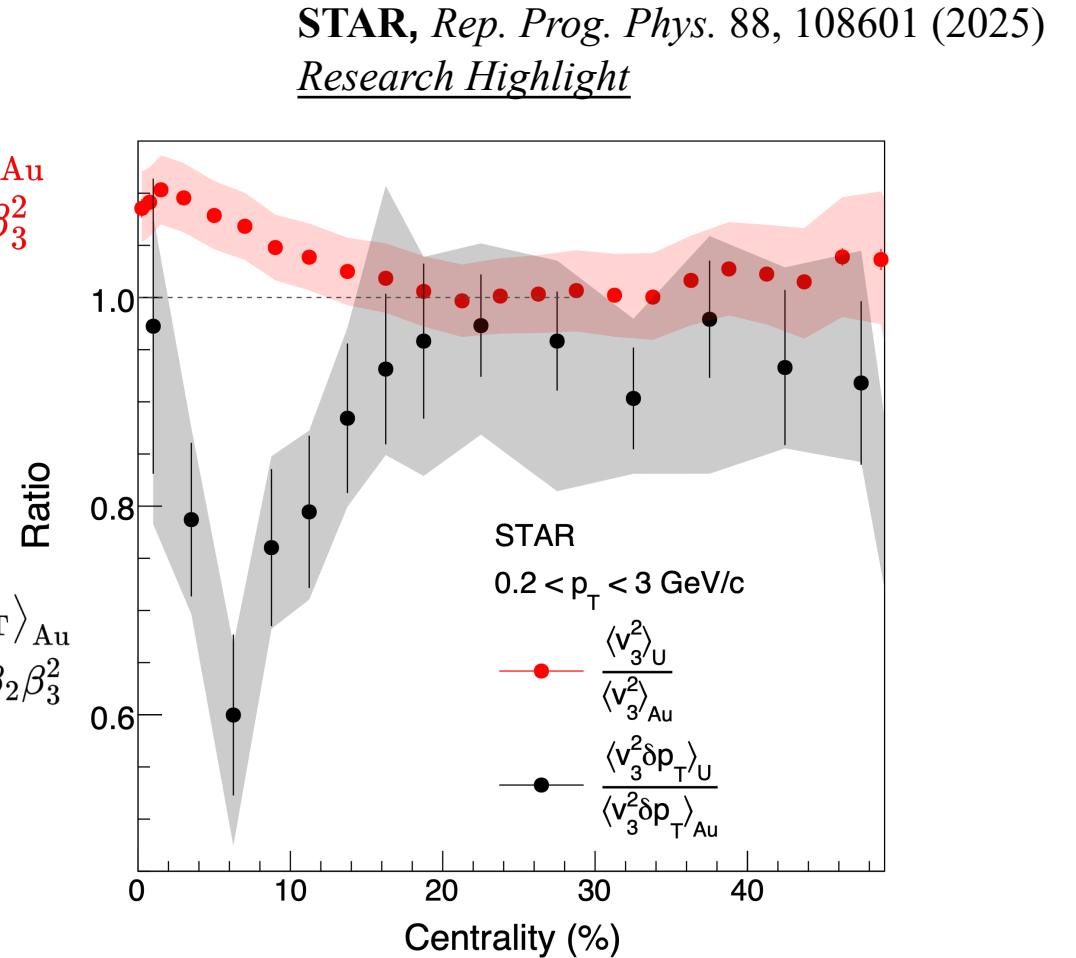


$$\langle v_3^2 \rangle_U > \langle v_3^2 \rangle_{Au}$$

$$R_{v_3^2} = a + b\beta_3^2$$

$$\langle v_3^2 \delta p_T \rangle_U < \langle v_3^2 \delta p_T \rangle_{Au}$$

$$R_{v_3^2 \delta p_T} = a - b\beta_2\beta_3^2$$



However, v_3 is fluctuation driven, expect in central

$$\langle v_3^2 \rangle \propto \langle \epsilon_3^2 \rangle \sim 1/A$$

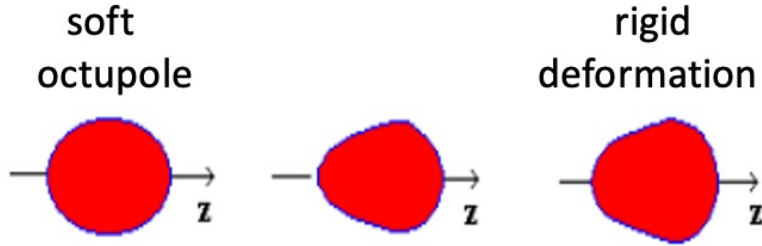
mass number \nearrow

- Order of v_3 and v_3 - p_T reversed by considering non-zero $\beta_{3,U}$, $\beta_{4,U}$.
- An evidence $\beta_{3,U}$ and modest $\beta_{3,U} \sim \beta_{4,U} \sim 0.08-0.10$ are confirmed

Probe $\beta_{3,U}$ and its fluctuation

L. Liu, C. Zhang, J. Chen, J. Jia, X. Huang, Y.-G. Ma, 2509.09376

Octupole “collectivity”



$$\langle \beta_3^2 \rangle = \bar{\beta}_3^2 + \sigma_{\beta_3}^2$$

Case	$\bar{\beta}_3$	σ_{β_3}	$\langle \beta_3^2 \rangle$	$\langle \beta_3^4 \rangle$
U _{case0}	0.00	0.100	0.01	0.000300
U _{case1}	0.05	0.087	0.01	0.000288
U _{case2}	0.06	0.080	0.01	0.000274
U _{case3}	0.07	0.071	0.01	0.000252
U _{case4}	0.08	0.060	0.01	0.000218
U _{case5}	0.09	0.044	0.01	0.000169
U _{case6}	0.10	0.000	0.01	0.000100

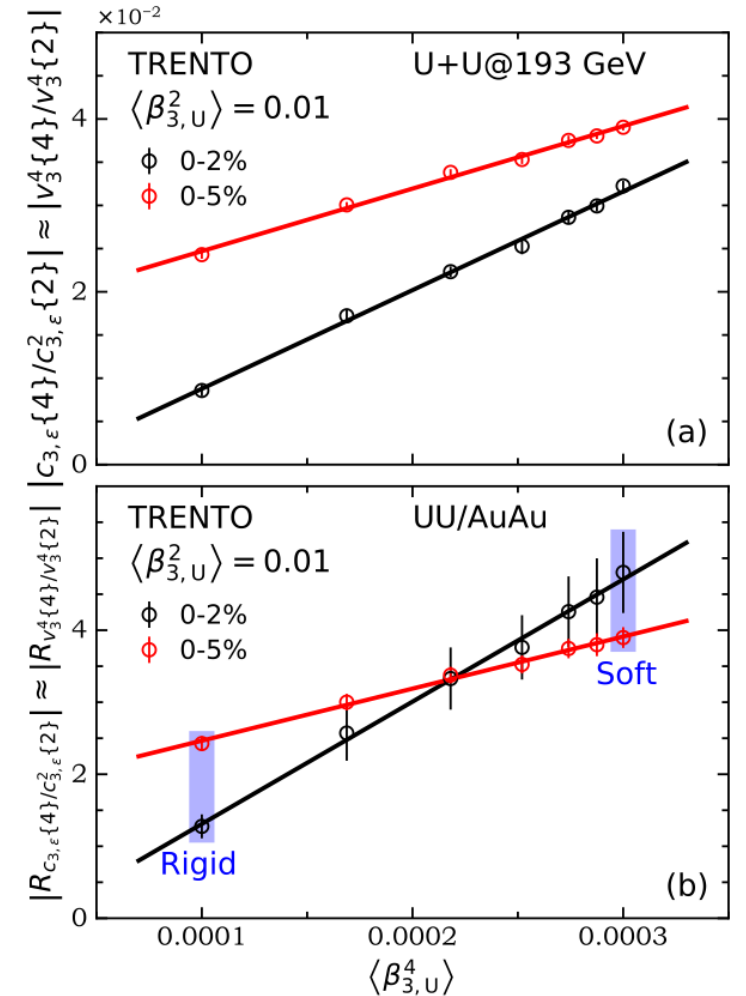
$$c_{n,\varepsilon}\{2\} = \langle \varepsilon_n^2 \rangle \approx \langle \varepsilon_{n,0}^2 \rangle + \langle p_n p_n^* \rangle \langle \beta_n^2 \rangle$$

$$c_{n,\varepsilon}\{4\} = \langle \varepsilon_n^4 \rangle - 2\langle \varepsilon_n^2 \rangle^2$$

$$\approx \langle \varepsilon_{n,0}^4 \rangle - 2\langle \varepsilon_{n,0}^2 \rangle^2 + \langle p_n^2 p_n^{2*} \rangle \langle \beta_n^4 \rangle - 2\langle p_n p_n^* \rangle^2 \langle \beta_n^2 \rangle^2$$

Four-particle correlation is linearly scaled to $\langle \beta_{3,U}^4 \rangle$.

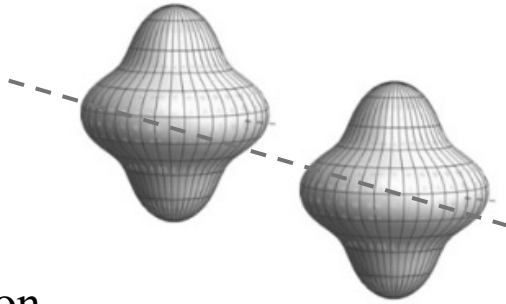
A way to discriminate between static and dynamic collective modes in high-energy nuclear collisions



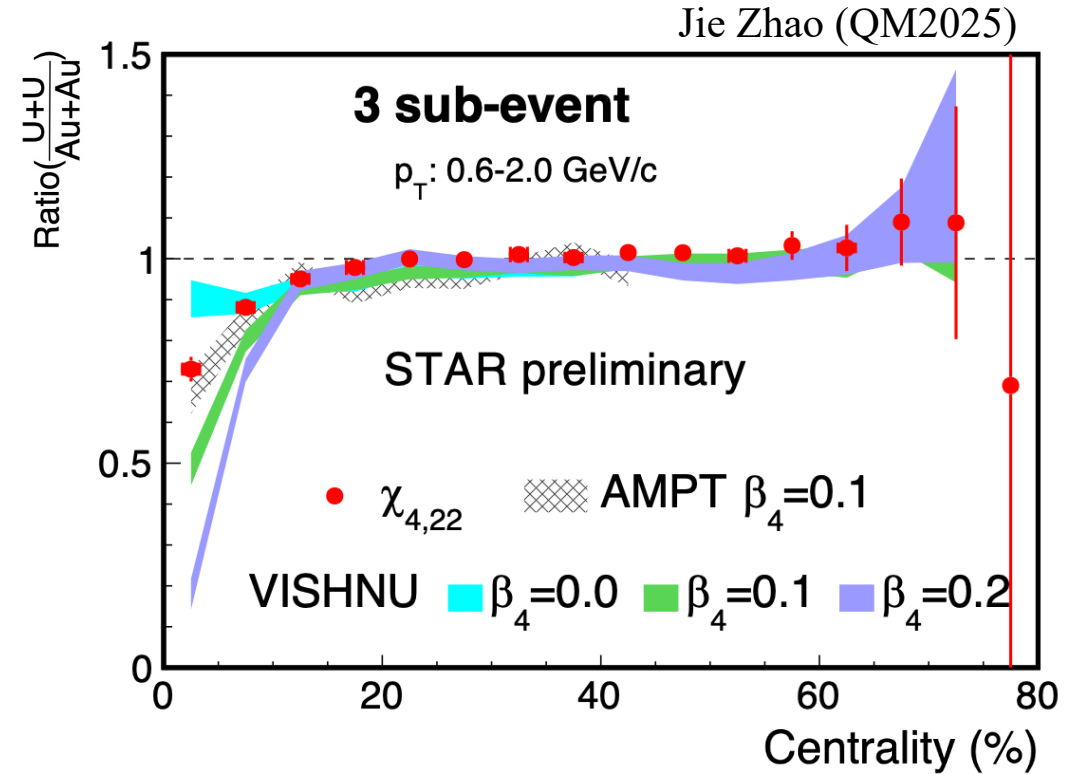
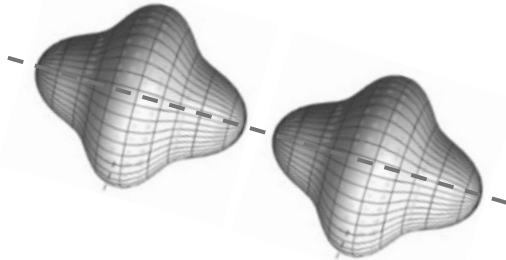
Evidence of hexadecapole deformation $\beta_{4,U}$

$\beta_{4,U}$ -induced geometry effect

Body-body configuration



Tip-tip configuration



Non-linear response coefficient is sensitive to the $\beta_{4,U}$

$\beta_{4,U}$ constrained using $\chi_{4,22}$ ratio in the central region

Model tuning is ongoing

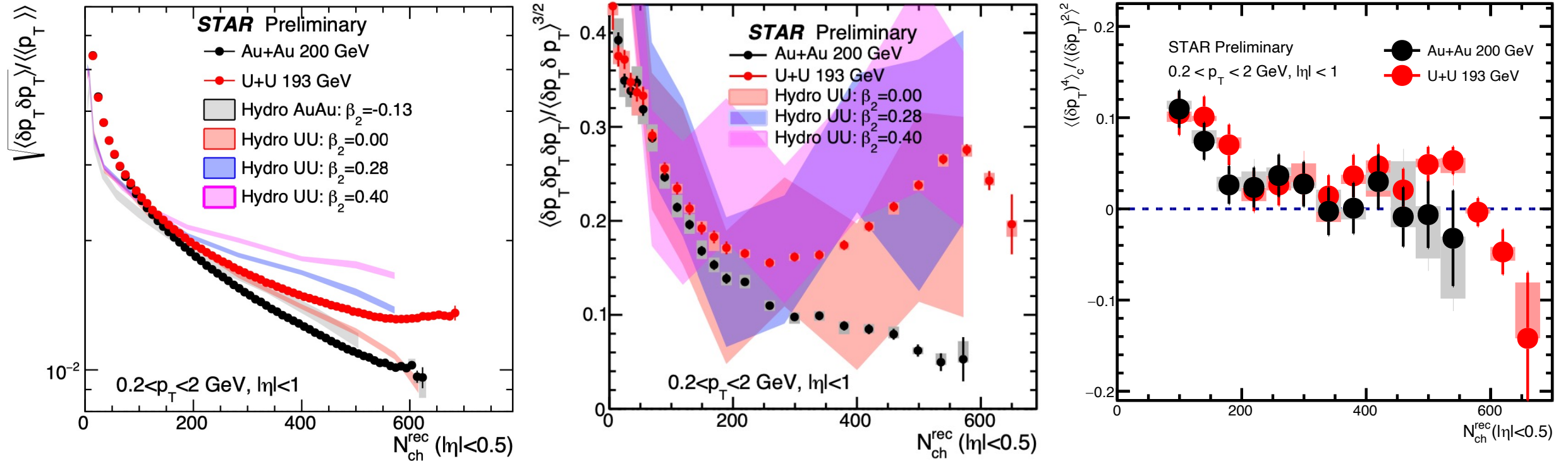
Z. Wang, J. Chen, H. Xu, J. Zhao, *PRC* 110, 034907 (2024)

H. Xu, J. Zhao, F. Wang, *PRL* 132, 262301 (2024)

W. Ryssens, G. Giacalone, B. Schenke, C. Shen, *PRL* 130, 212302 (2023)

[p_T] fluctuations and comparisons to hydro model

C. Zhang, *INT2023*, *WWND2023*



Au+Au: variance and skewness follow independent source scaling $1/N_s^{n-1}$ within power-law decrease

U+U: large enhancement in normalized variance and skewness and sign-change in normalized kurtosis
 → size fluctuations enhanced

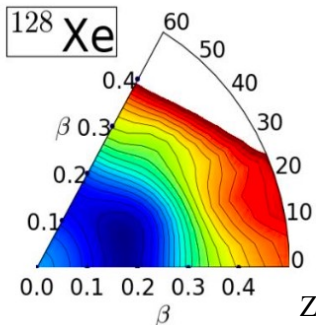
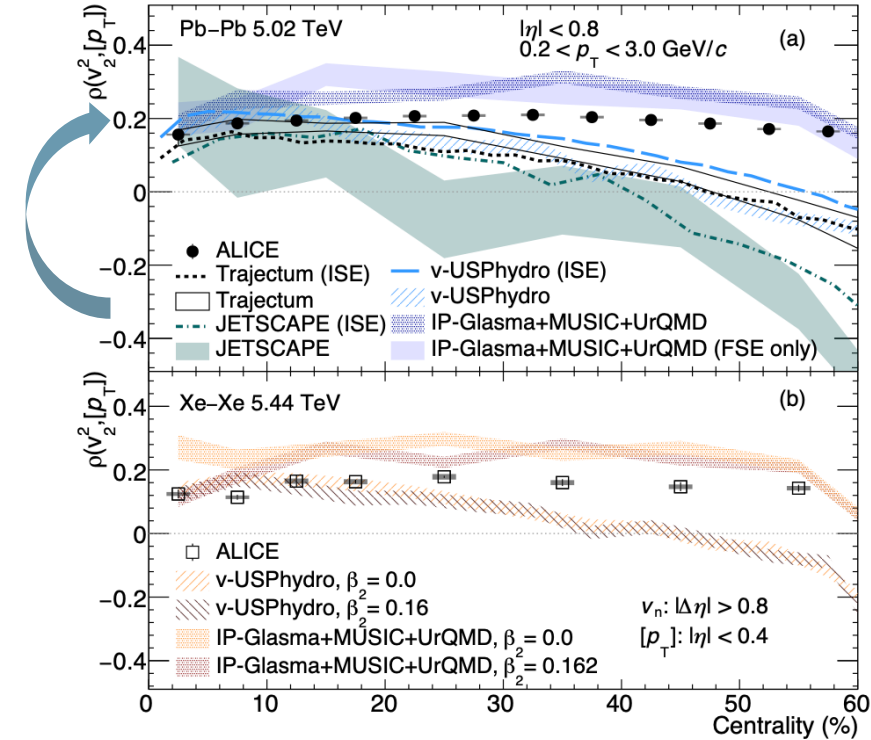
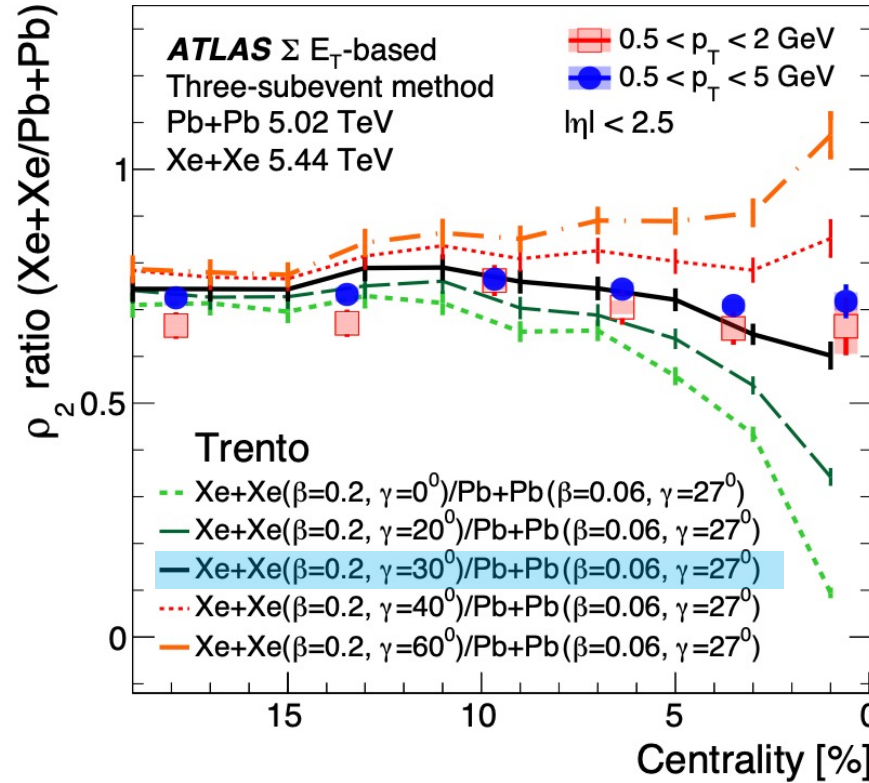
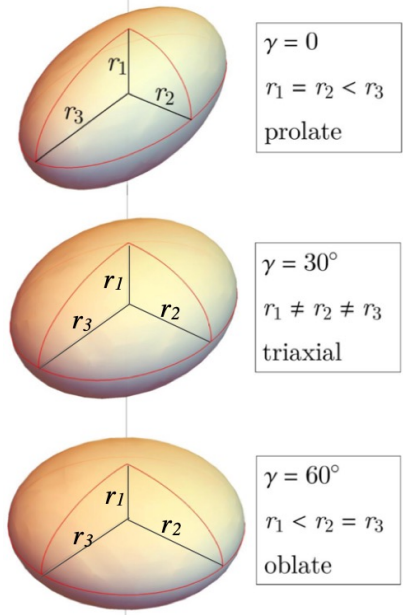
The nuclear deformation role is further confirmed by hydro calculations. But we need more statistics.

[p_T] fluctuations also serve as a good observable to explore the role of nuclear deformation.

Shape of ground-state ^{129}Xe : $\beta_{2,\text{Xe}}$ and γ_{Xe}

ATLAS, *PRC* 107, 054910 (2023)

ALICE, *PLB* 834, 137393 (2022)



γ -soft (flat distribution in $0 \leq \gamma \leq 60^\circ$)

Z.P. Li et al., *PRC* 81, 034316 (2010)

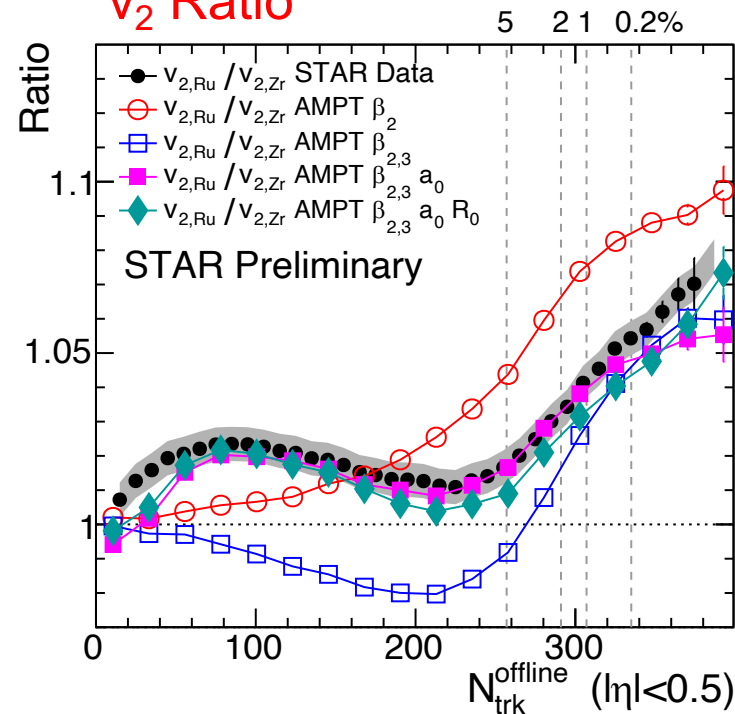
- Pave a novel way to characterize the QGP initial state
- The medium effect was mostly canceled.
- Study the triaxial shape of ^{129}Xe nuclei

S. Zhao, H. Xu, Y. Zhou, Y. Liu, H. Song, *PRL* 133, 192301 (2024)

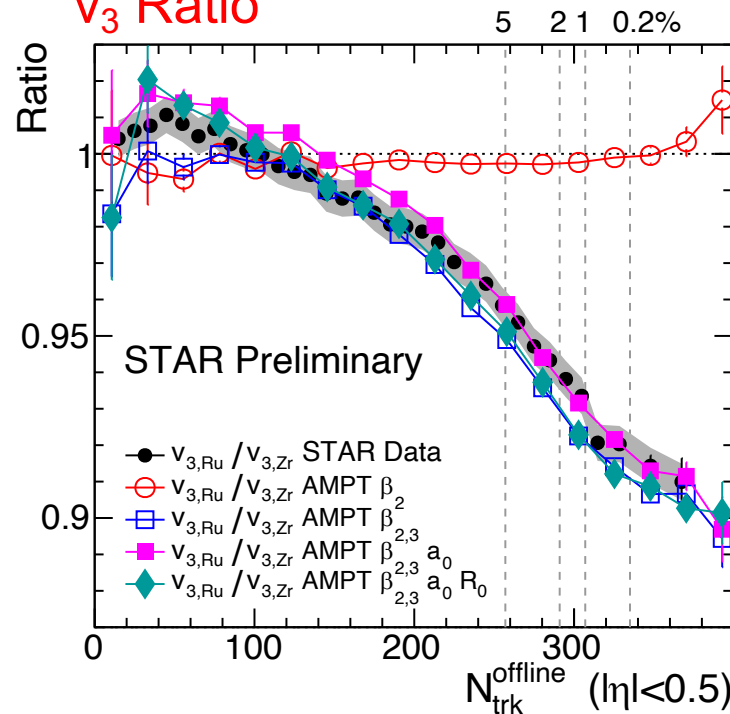
A. Dimri, S. Bhatta, J. Jia, *EPJA* 59 45(2023)

Nuclear structure in isobar ^{96}Ru and ^{96}Zr $\frac{\mathcal{O}_{^{96}\text{Ru}} + \mathcal{O}_{^{96}\text{Ru}}}{\mathcal{O}_{^{96}\text{Zr}} + \mathcal{O}_{^{96}\text{Zr}}} \stackrel{?}{=} 1$

v_2 Ratio



v_3 Ratio

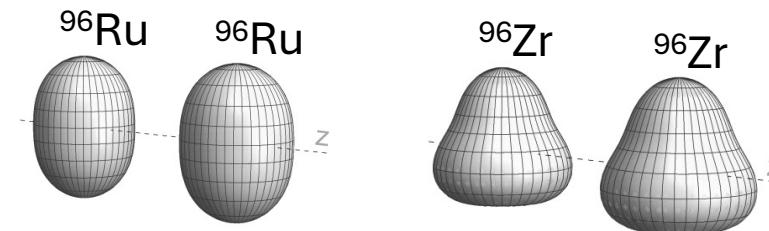


$\beta_{2,\text{Ru}} \sim 0.16$ increase v_2 , no influence on v_3 ratio

$\beta_{3,\text{Zr}} \sim 0.2$ decrease v_2 in mid-central, decrease v_3 ratio

$\Delta a_0 = -0.06$ fm increase v_2 mid-central, small impact on v_3

Radius $\Delta R_0 = 0.07$ fm only slightly affects v_2 and v_3 ratio.



$$\beta_{2,\text{Ru}} = 0.16 \pm 0.02 \quad \beta_{3,\text{Zr}} = 0.20 \pm 0.02$$

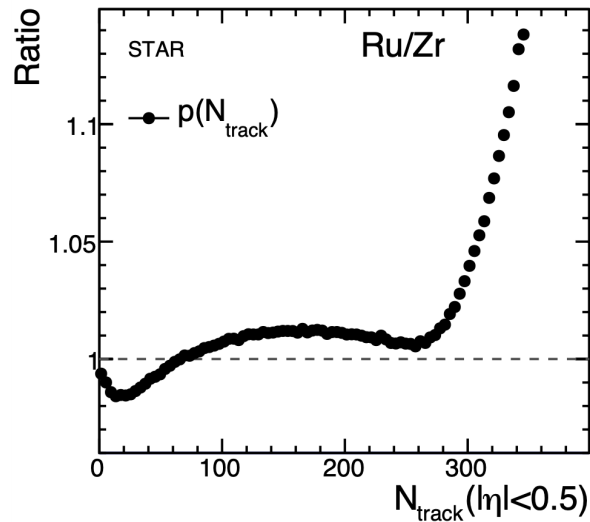
difference	$\Delta\beta_2^2$	$\Delta\beta_3^2$	Δa_0	ΔR_0
	0.0226	-0.04	-0.06 fm	0.07 fm

Current estimation is from transport model

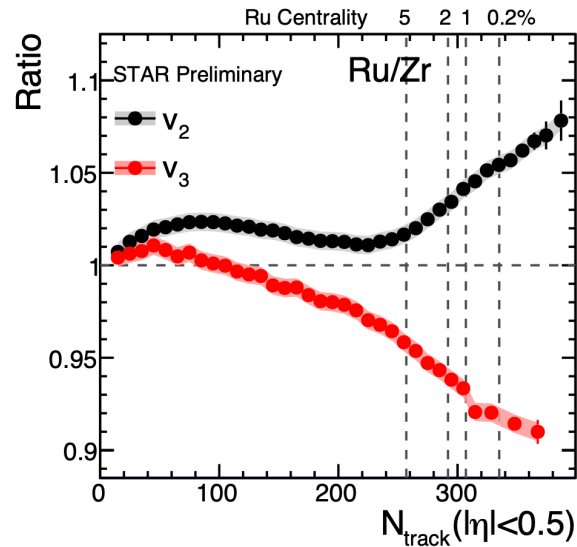
- Direct observation of octupole deformation in ^{96}Zr nucleus
- Imply the neutron skin difference between ^{96}Ru and ^{96}Zr
- Simultaneously constrain parameters using Bayesian analysis

$$R_{\mathcal{O}} \equiv \frac{\mathcal{O}_{\text{Ru}}}{\mathcal{O}_{\text{Zr}}} \approx 1 + c_1 \Delta\beta_2^2 + c_2 \Delta\beta_3^2 + c_3 \Delta R_0 + c_4 \Delta a_0$$

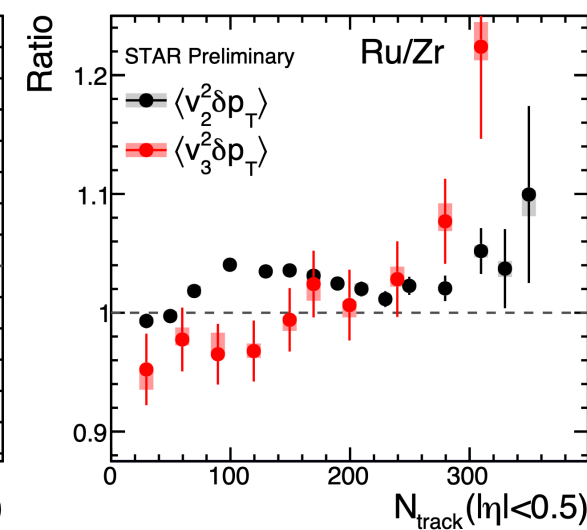
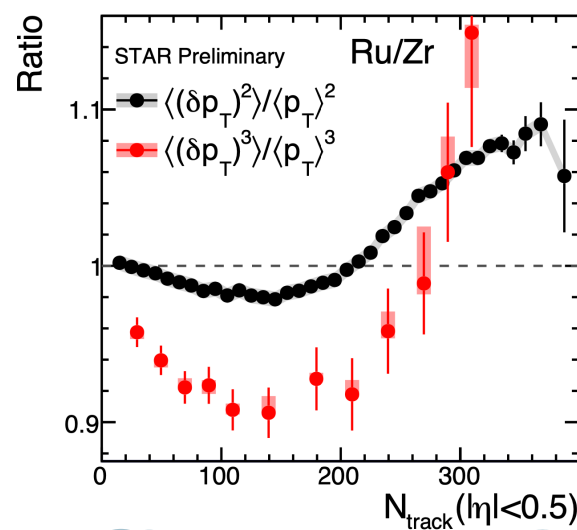
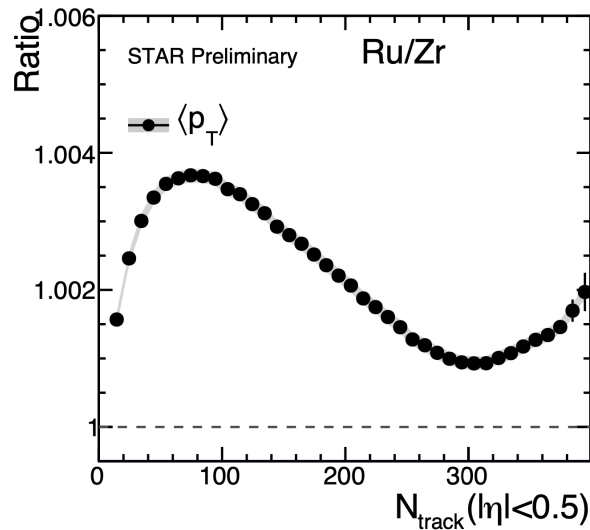
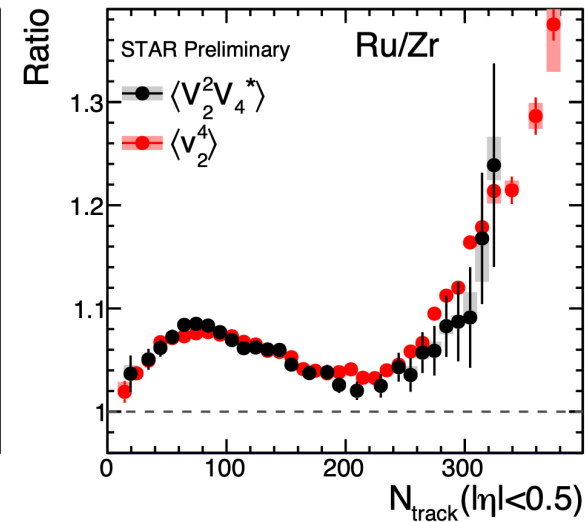
One-body distribution



Two-body correlations



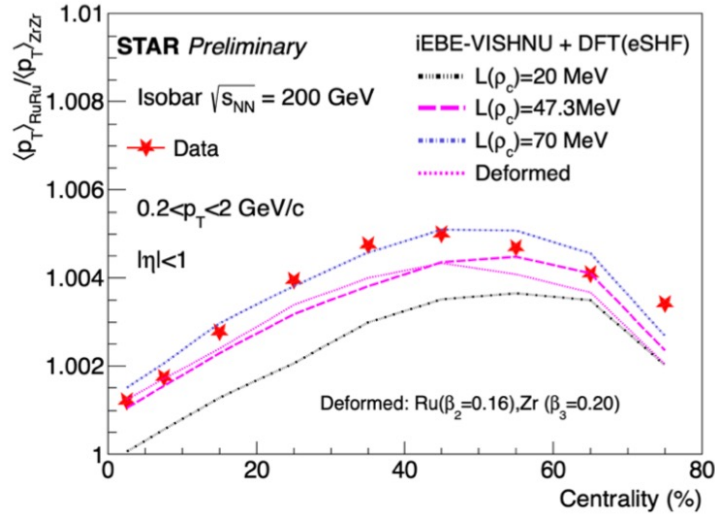
Three-body correlations



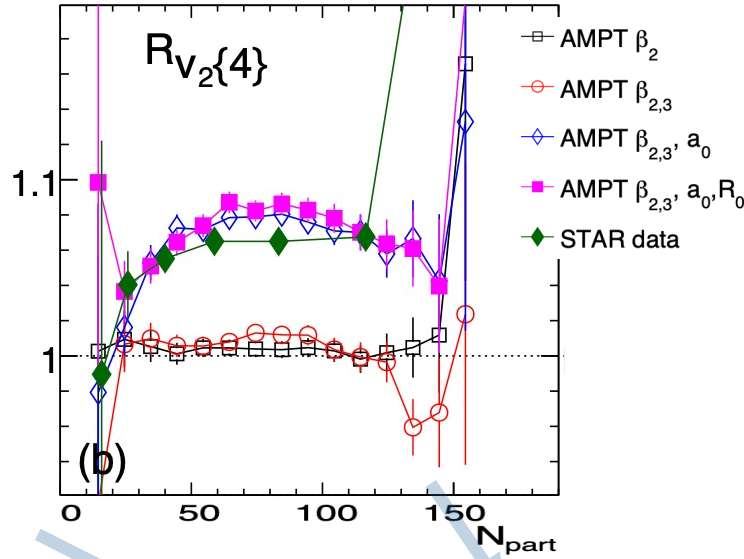
Imaging the radial structures (neutron skin)

Radial parameters R_0, a_0 are properties of one-body distribution $\rightarrow \langle p_T \rangle, \langle N_{ch} \rangle, v_2^{RP} \sim v_2\{4\}, \sigma_{tot}, ZDC$

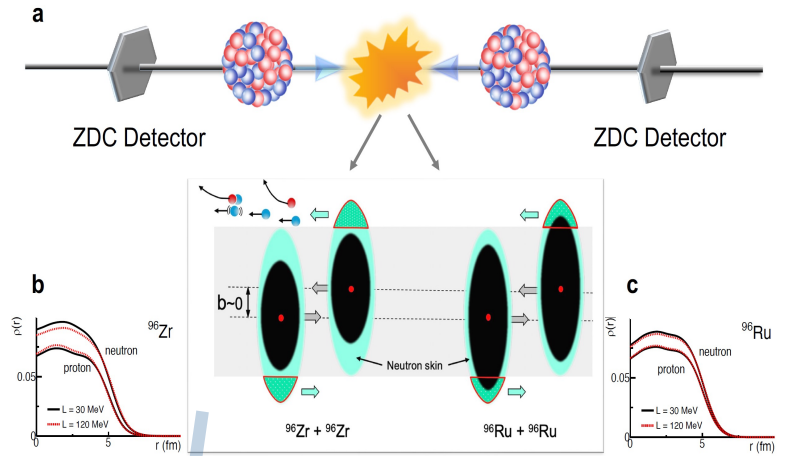
H. Xu, *QM2023*



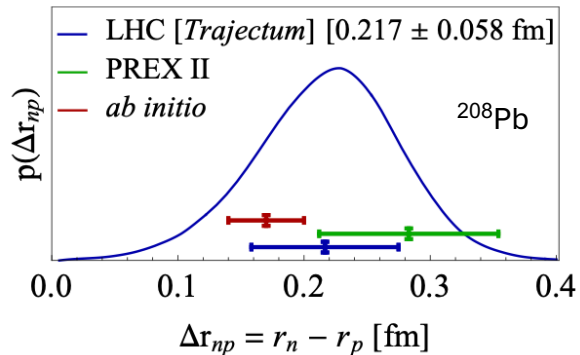
J. Jia, G. Giacalone, C. Zhang, *PRL 131, 022301 (2023)*



L. Liu, J. Xu et al., *PLB 834, 137441 (2022)*
PRC 106, 034913 (2022)

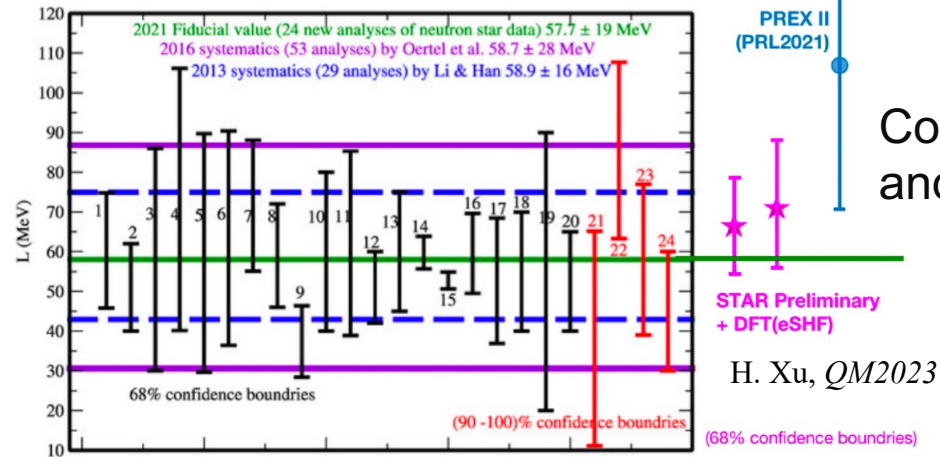


PREX- CREX puzzle in nuclear physics



G. Giacalone, G. Nijs, W. Schee, *PRL 131, 202302 (2023)*

B. Li, et.al Universe 7, 182 (2021)



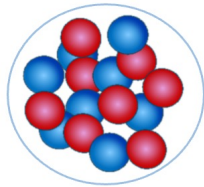
PREX II (PRL2021)

Constrain neutron skin and symmetry energy

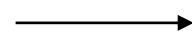
H. Xu, *QM2023*

III. Nucleonic cluster pattern in light nuclei

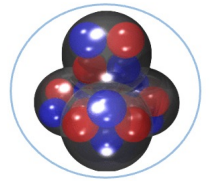
--- from one-body distribution to many-body nucleon correlations



$$\rho(r) \propto \frac{1 + w(r^2/R^2)}{1 + e^{(r-R)/a_0}}$$

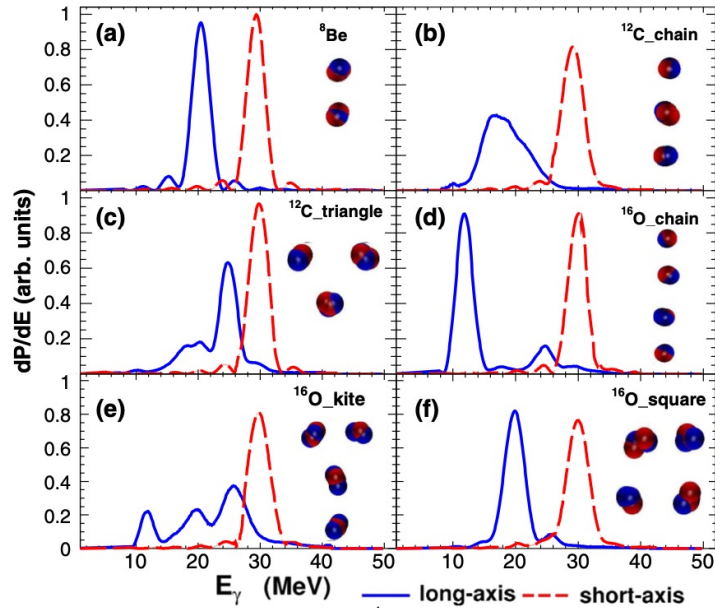


Modern *ab initio* first-principle calculations

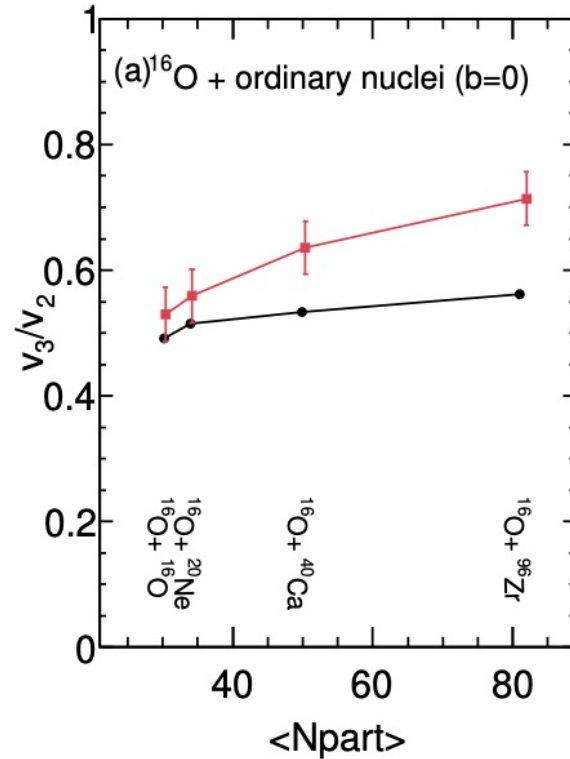


Pioneer theory instructions of the nucleonic clustering

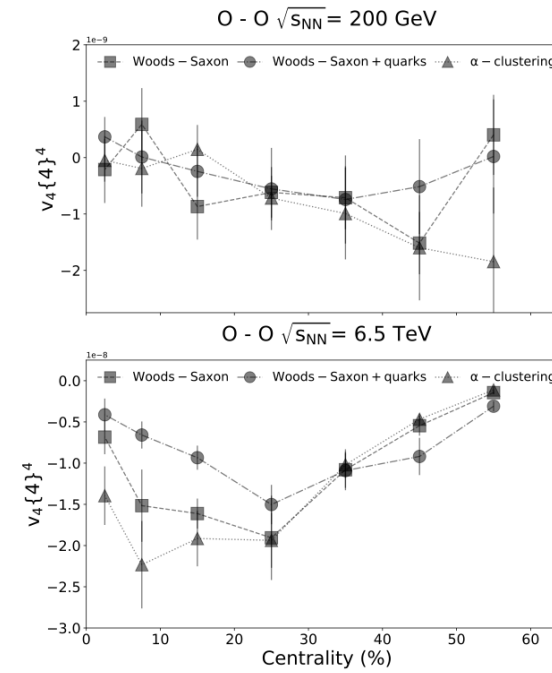
“Double magic number” in $^{16}_8\text{O}$ nuclei, possible alpha cluster in low-energy studies.



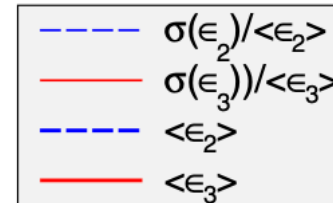
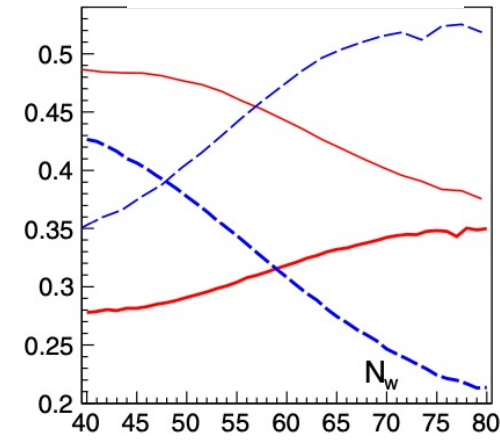
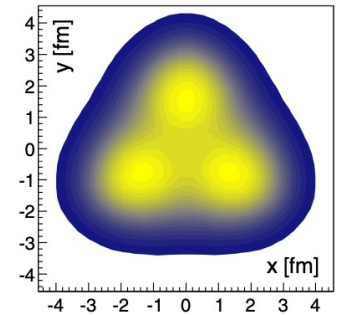
W. He, Y.-G. Ma et al., *PRL* 113, 032605 (2014)



Y.-G. Ma and S. Zhang, *Handbook of Nuclear Physics*, 2206.08218



Nicholas et al., *PRC* 104, L041901 (2021)



W. Broniowski, E. Arriola, *PRL* 112, 112501 (2014)

- ^{16}O nucleus could have different intrinsic topological structures.
- The initial configurations straightforwardly affect the final state observables in high energies.

Nucleon-nucleon correlations in finite quantum many-body systems

Possible cluster in ground-state $^{16}_8\text{O}$ nuclei in low energy

1) *Woods-Saxon: without many-body nuclear correlation*

2) *Nuclear Lattice Effective Field theory (NLEFT):
model with many-nucleon correlation including α clusters*

Lu et al., *PLB* 797, 134863 (2019)

M. Freer et al., *Rev. Mod. Phys.* 90, 035004 (2018)

S. Elhatisari et al., *Nature* 630, 59 (2024)

3) *Variational auxiliary field diffusion Monte Carlo (VMC):*

MC solution of Schrödinger eq. from the time evolution of trial wave function.

A. Lonardononi et al., *PRC* 97, 044318 (2018)

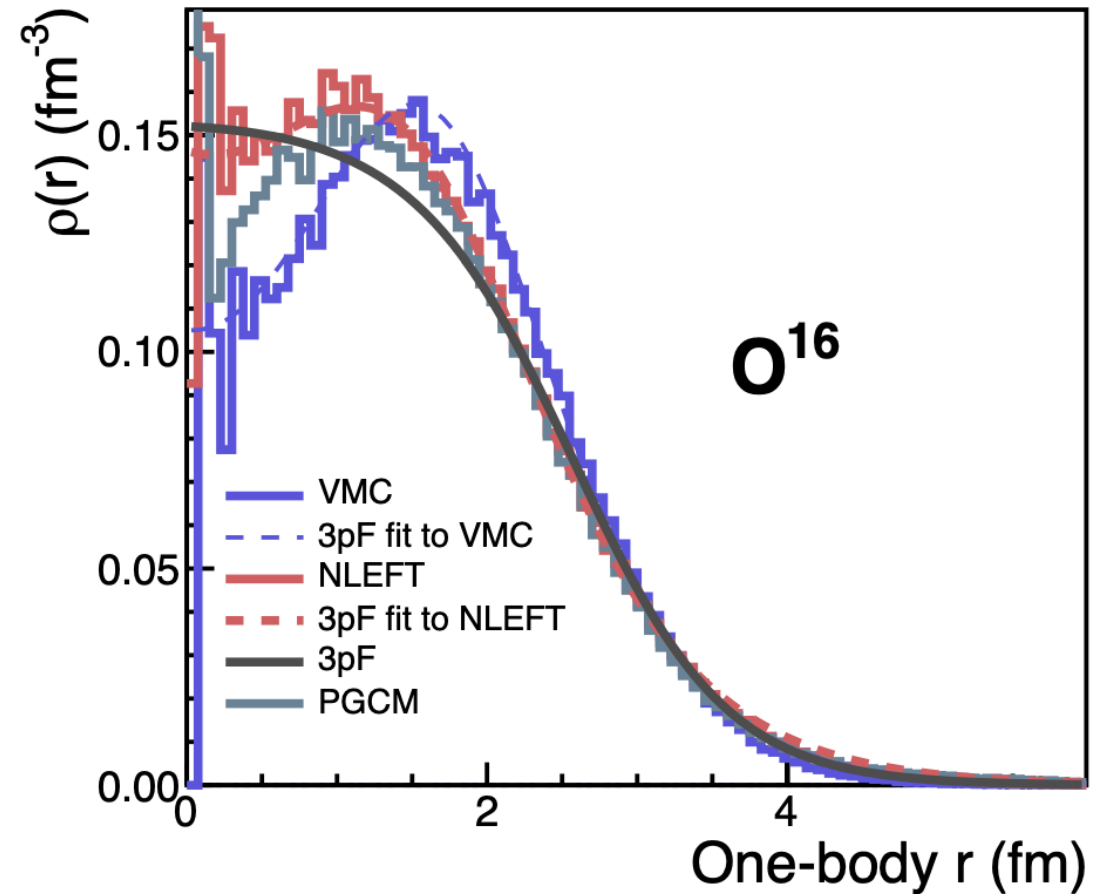
J. Carlson and R. Schiavilla, *Rev. Mod. Phys.* 70, 743 (1998)

4) *ab-initio Projected Generator Coordinate Method (PGCM):*

Wave function from variational calculation (as in density functional theory)

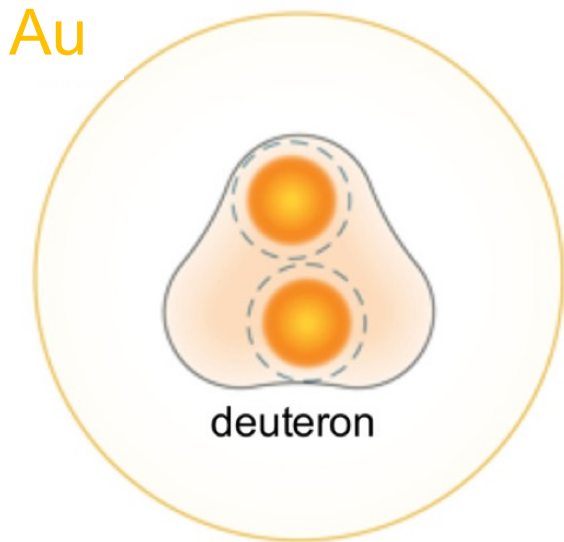
Frosini et al., *EPJA* 58, 62 (2022); *EPJA* 58, 63 (2022); *EPJA* 58, 64 (2022)

5) *Some other micro models...*



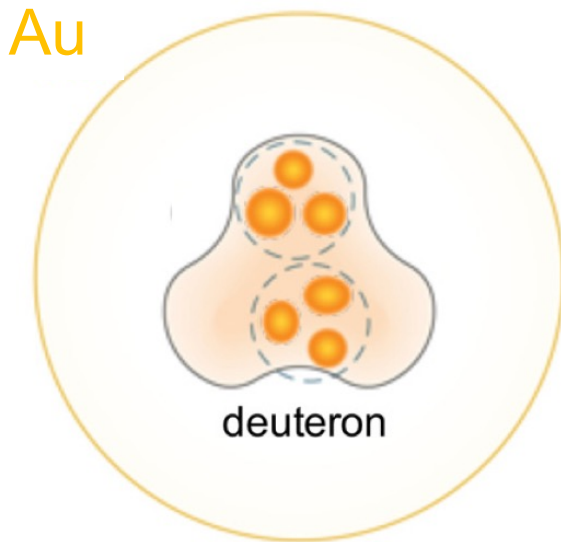
Nucleon/sub-nucleon fluctuation vs. nucleon-nucleon correlations

Nucleon fluctuation

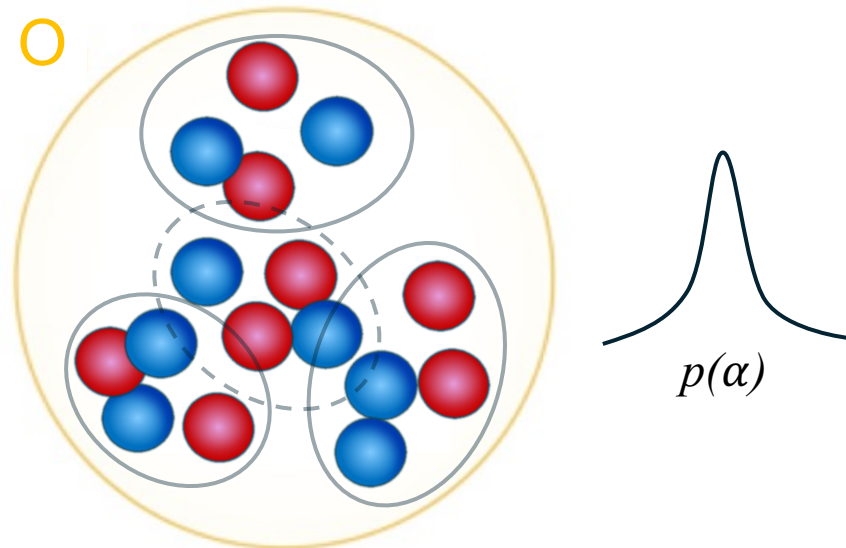


STAR, *PRL* 130, 242301 (2023)
STAR, *PRC* 110, 064902 (2024)

subnucleon fluctuation



NN correlation (cluster pattern)



ab initio calculations

Y.-G. Ma, S. Zhang, *Handbook of Nuclear Physics* (2022)
 C. Zhang, J. Chen, G. Giacalone, S. Huang, J. Jia, Y.-G. Ma, *PLB* 862, 139322 (2025)
 S. Huang, J. Jia, C. Zhang, *PLB* 870, 139926 (2025)
 X. Zhao, G. Ma, Y. Zhou, Z. Lin and C. Zhang, *PLB* 874, 140254 (2026)
 P. Li, B. Zhou, G.-L. Ma, *PRL* 136, 082302 (2026)
 S. Jahan, Roch, C. Shen, *PRC* 113, 024919 (2026)
 Y. Wang, S. Zhao, B. Cao, H. Xu and H. Song, *PRC* 109, L051904 (2024)
 H. Wang, S. Li, J. Xu, Z. Ren, *PLB* 866, 139516 (2025)
 J. Hu, H. Xu, X. Wang, S. Pu, 2507.01493

d+Au collision, 200 GeV

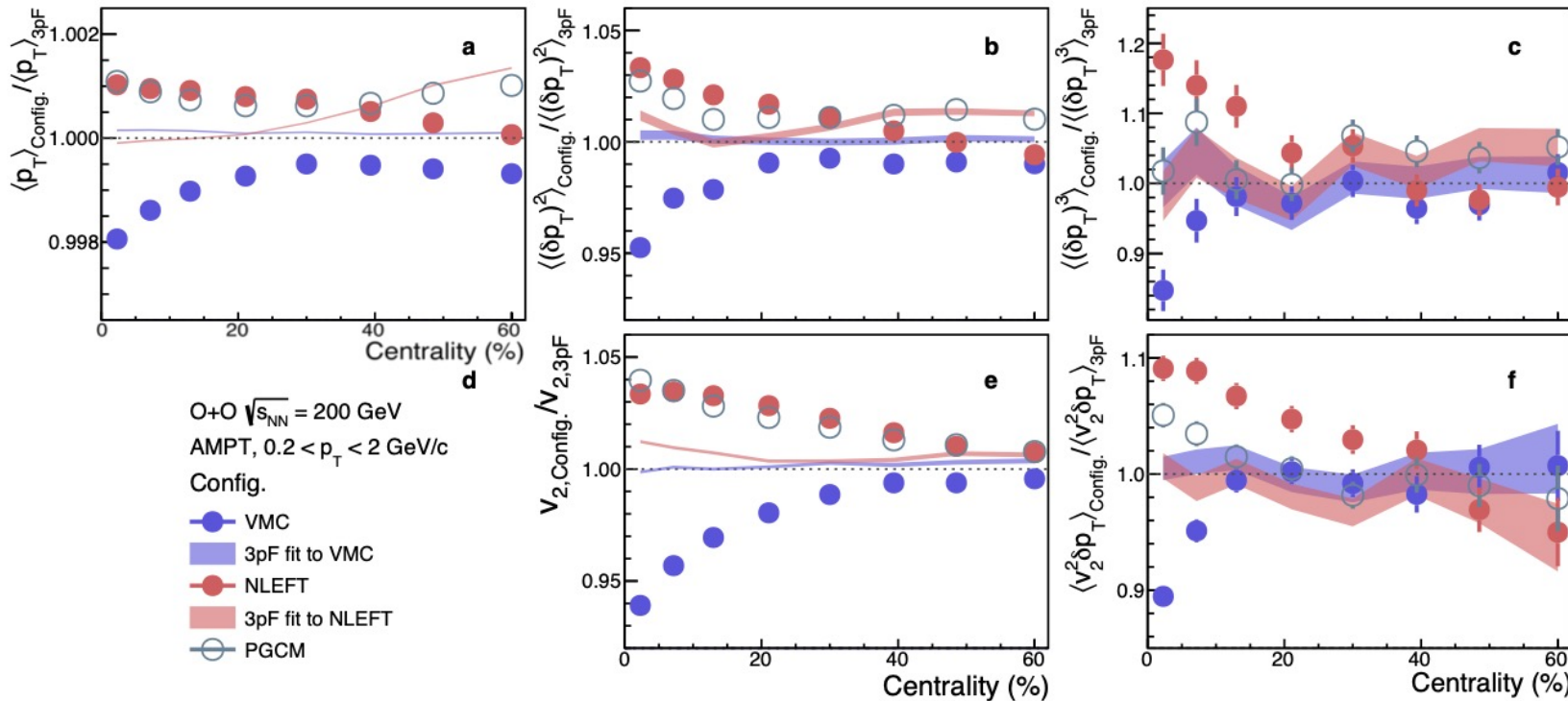
Nearly same N_{ch}

O+O collision, 200 GeV

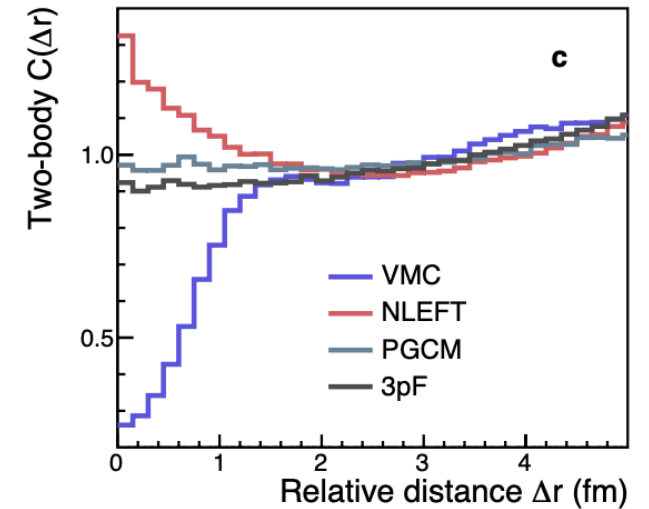
Ab-initio nucleon-nucleon correlations and their impact on high-energy

C. Zhang, J. Chen, G. Giacalone, S. Huang, J. Jia, Y.-G. Ma, *PLB* 862, 139322 (2025)

Multiple final-state observables



Two-body correlations in coordinate space

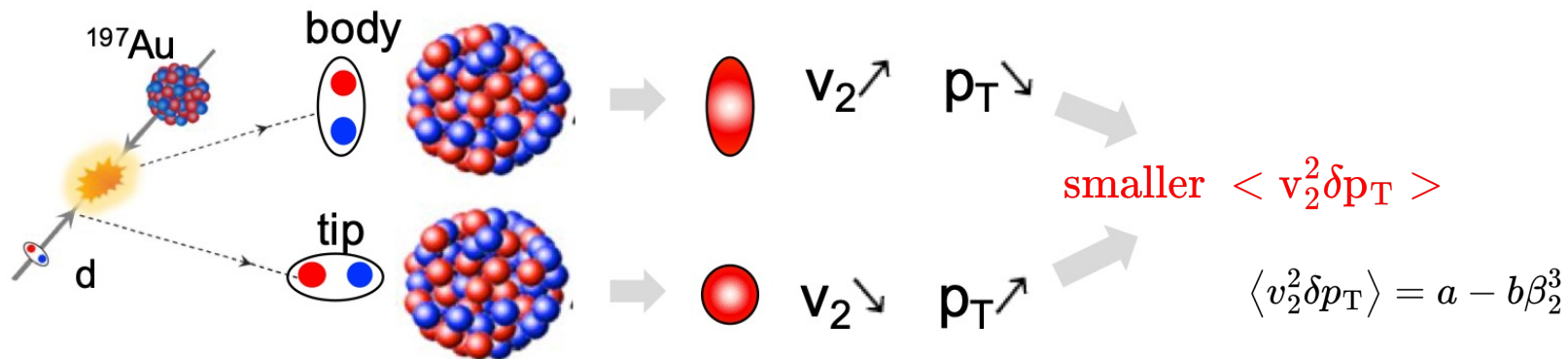


$$C(\Delta r) = \frac{\int d^3s f(\mathbf{s} + \frac{\mathbf{r}}{2}, \mathbf{s} - \frac{\mathbf{r}}{2})}{\int d^3s f(\mathbf{s} + \frac{\mathbf{r}}{2}) f(\mathbf{s} - \frac{\mathbf{r}}{2})}$$

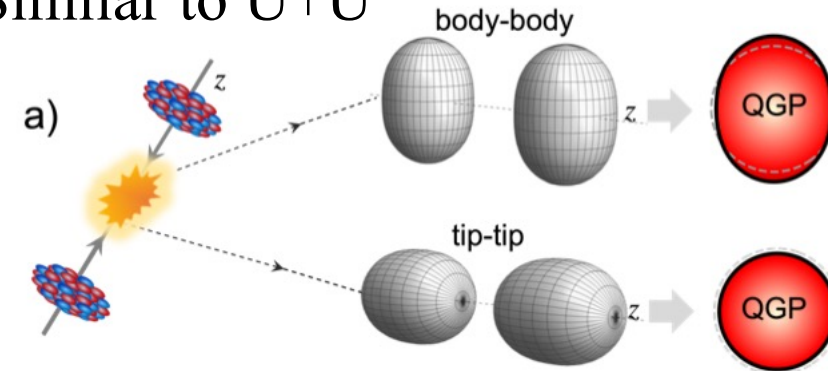
- 3pF as the baseline can NOT capture the NN correlations.
- Distinct differences are observed between VMC and NLEFT/PGCM.
- Central collision is prominent.

Impact of prolate shape of deuteron and the underlying Oxygen structure

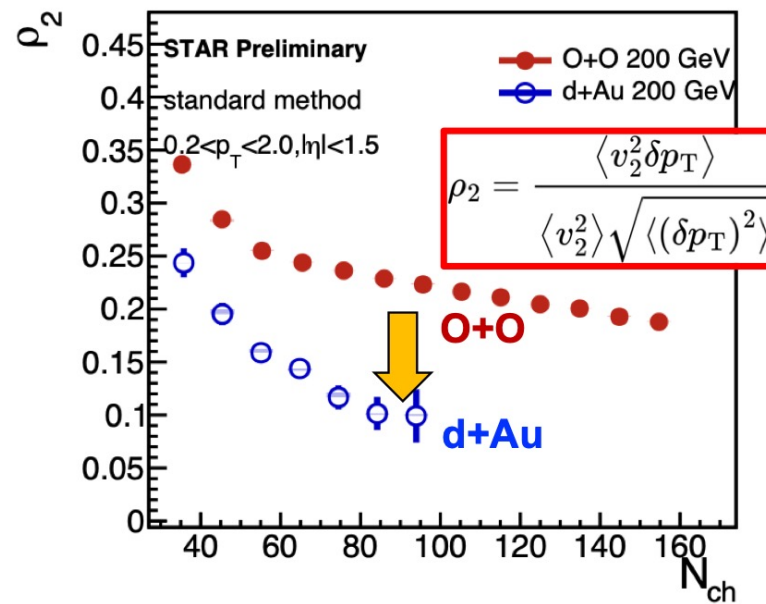
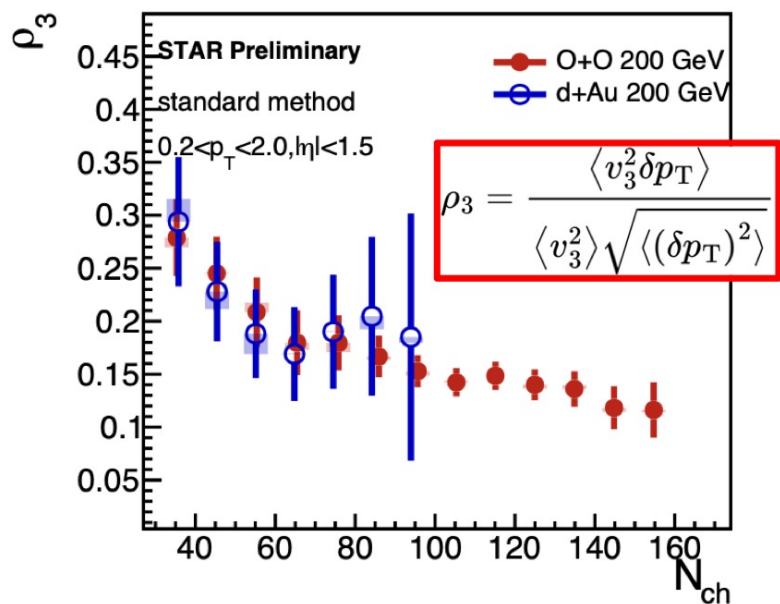
J. Jia, Z. Wang, sQM2026



Similar to U+U



STAR, *Rep. Prog. Phys.* 88, 108601 (2025)



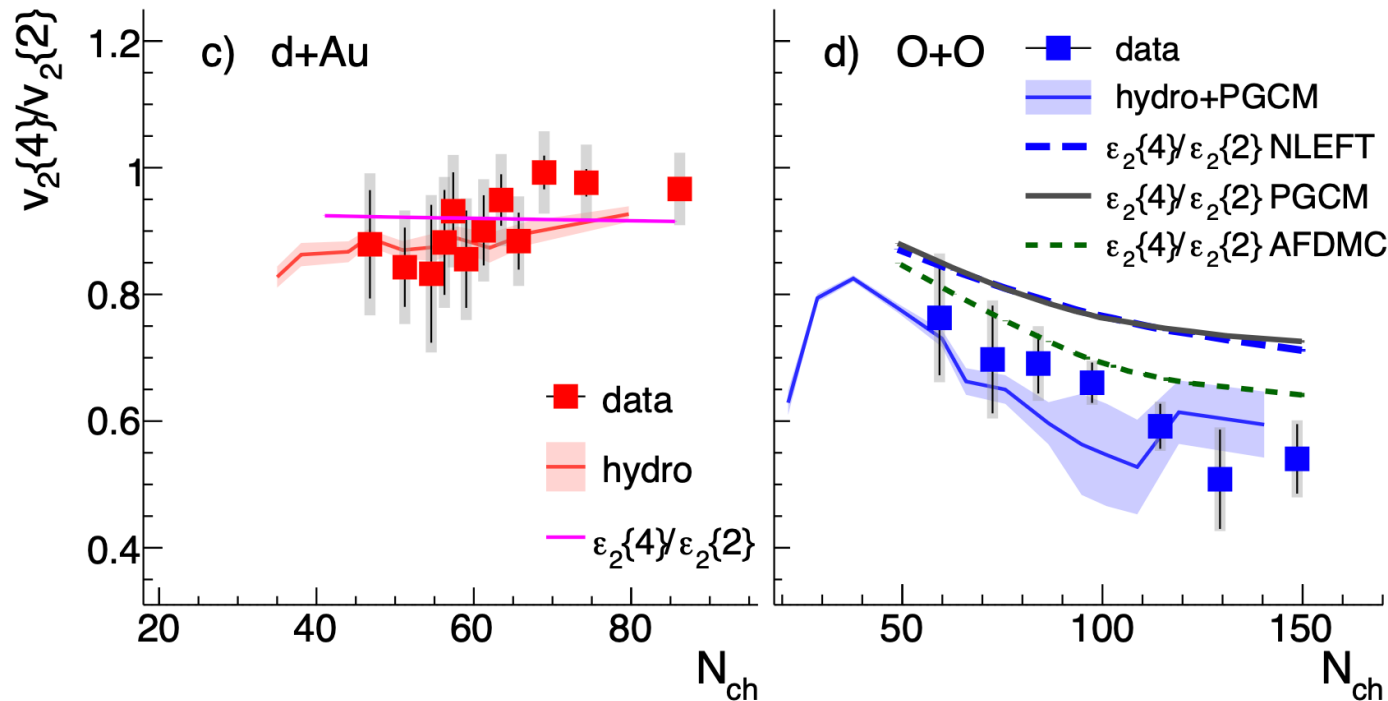
The deuteron wave function is fixed.

^{16}O structure might be important.

Behavior of $\langle v_2^2 \delta p_T \rangle$ consistent with QGP response to the prolate shape of deuteron

Benchmarking geometric tomography of ^{16}O nucleus

STAR, 2510.19645



S. Jahan, Roch, C. Shen, *PRC* 113, 024919 (2026) NLEFT from D. Lee, PGCM from B. Bally, T. Duguet

Small fluctuation in d+Au

$$\frac{v_2^{dAu}\{4\}}{v_2^{dAu}\{2\}} \approx \frac{\varepsilon_2^{dAu}\{4\}}{\varepsilon_2^{dAu}\{2\}} \approx 0.9$$

large fluctuation in O+O

$$\frac{v_2^{OO}\{4\}}{v_2^{OO}\{2\}} \approx \frac{\varepsilon_2^{OO}\{4\}}{\varepsilon_2^{OO}\{2\}} \sim 0.6$$

d+Au is flat; Large enhancement in O+O with continuous decrease

$\varepsilon_2\{4\} / \varepsilon_2\{2\}$ from three models:

AFDMC vs. EFT/PGCM has a visible difference.

Nucleon-nucleon correlations impact initial-state fluctuations.

C. Zhang et al., *PLB* 862, 139322 (2025)

G. Giacalone, B. Bally, W. Zhao et al., *PRL* 135, 012302 (2025), *PRL* 134, 082301 (2025)

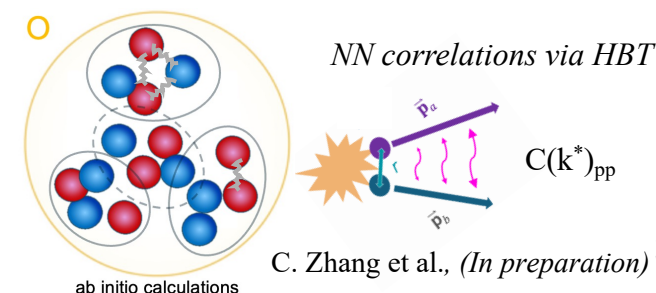
The interplay between nucleon/sub-nucleon fluctuation and many-nucleon correlation.

STAR, *PRL* 130, 242301 (2023)

S. Huang, J. Jia, C. Zhang, *PLB* 870, 139926 (2025)

Geometric scan elucidates nuclear tomography and strong nuclear force?

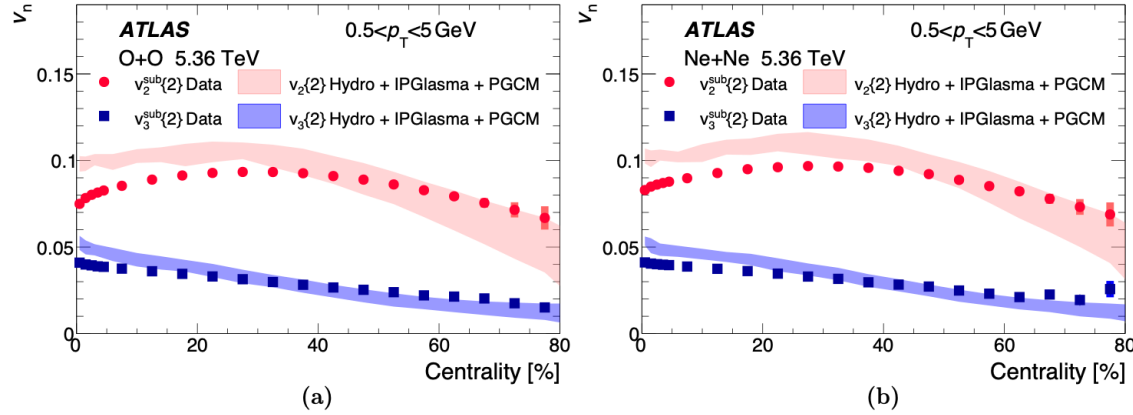
data & high-energy model & low-energy inputs



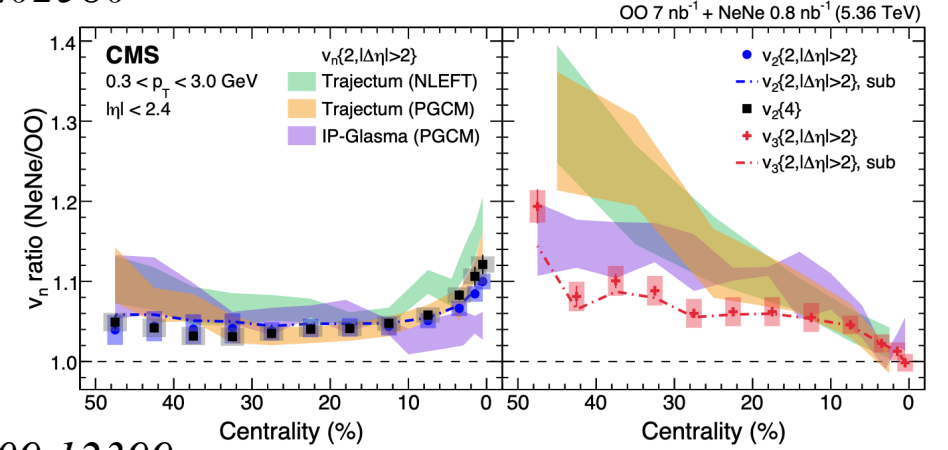
C. Zhang et al., (In preparation) 30

Flow ratios in ATLAS, ALICE, CMS, and LHCb results

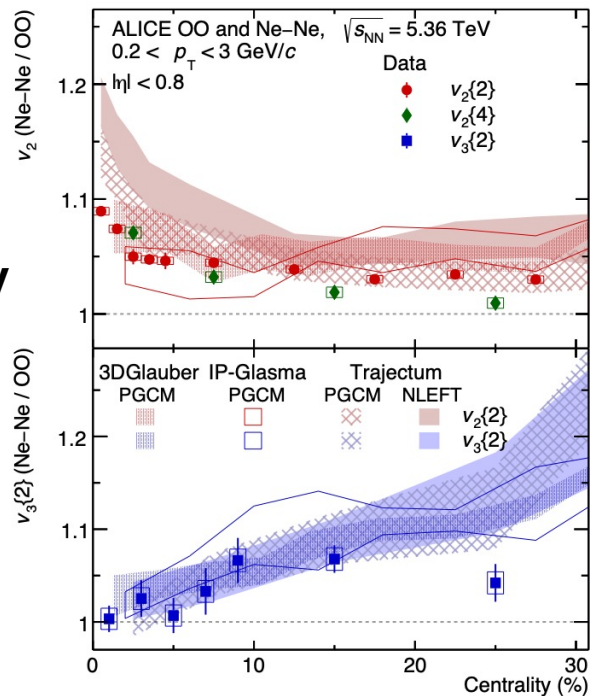
ATLAS, 2509.05171



CMS, 2510.02580

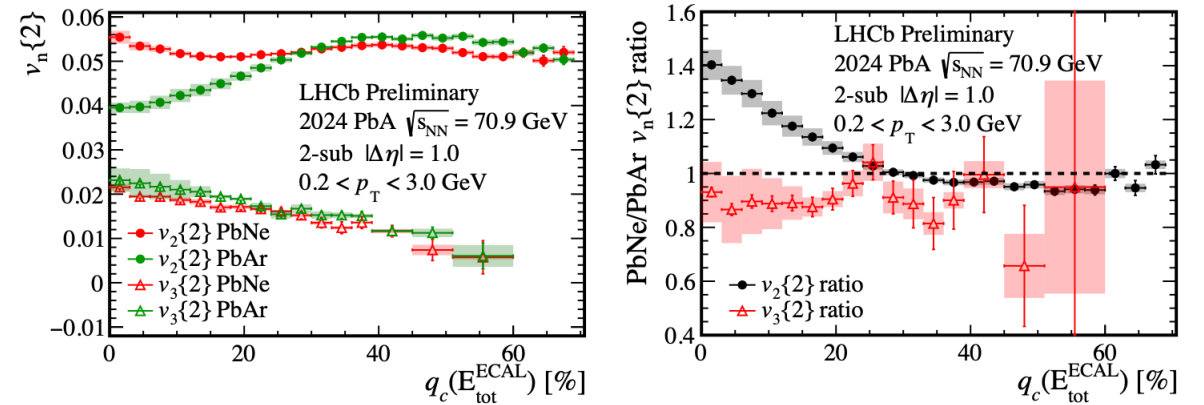


ALICE, 2509.06428



v_2 ratios (Ne/O) are largely enhanced in UCC.

LHCb, 2509.12399



New avenue: shape imaging method for light ions

G. Giacalone, B. Bally, G. Nijs et al., *PRL* 135, 012302 (2025)

G. Giacalone, W. Zhao, C. Shen et al., *PRL* 134, 082301 (2025)

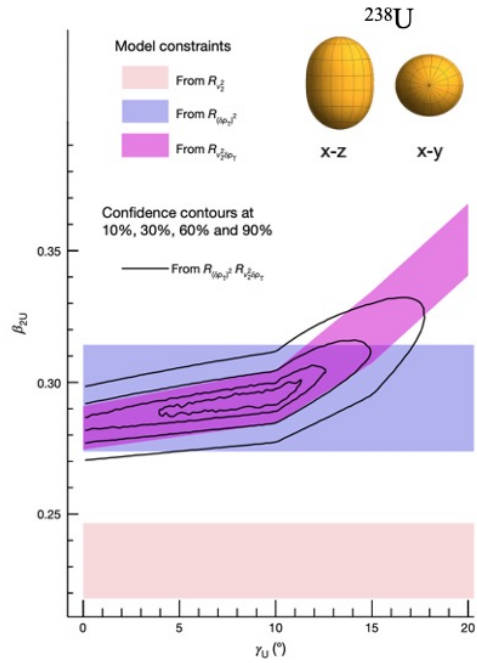
P. Li, B. Zhou, G.-L. Ma, *PRL* 136, 082302 (2026)

...

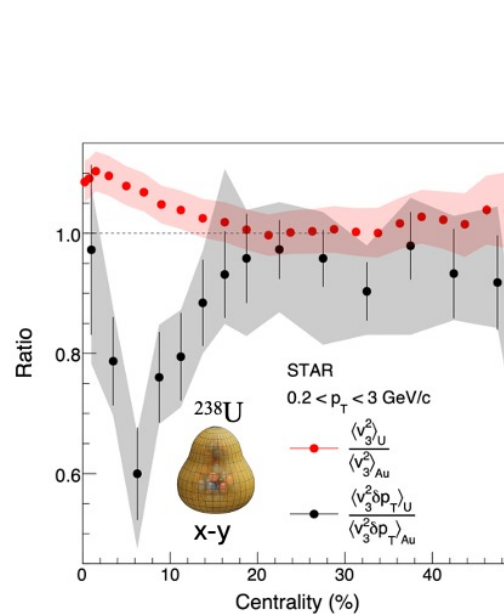
IV. Conclusions and Outlooks

1. The signatures of nuclear structure from large to small nuclear collisions are ubiquitous:

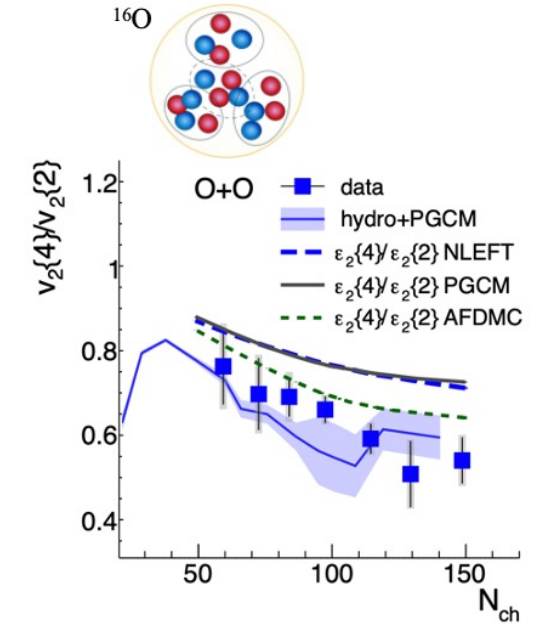
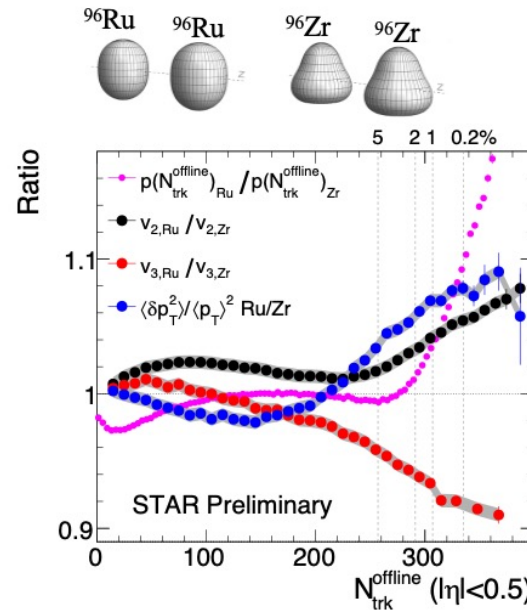
STAR, *Nature* 635, 67-72 (2024)



STAR, *Rep. Prog. Phys.* 88, 108601 (2025)



STAR, 2510.19645

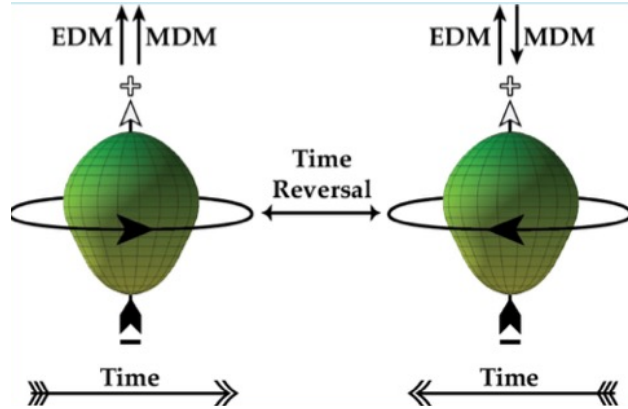


2. Many potential applications :

- Rigid and soft β_n and γ (shape fluctuations/coexistence)
- Neutron skin & symmetry energy constraints
- Confronted with ab initio calculations and more light-ion studies
- Intersection with Nucleosynthesis, nuclear fission, $0\nu\beta\beta$
- Energy evolutions in TeV-GeV facilities, LHC, HIAF, NICA, FAIR, SPS, NA61
- Other tools, i.e. UPC, AI-assistant work

IV. Conclusions and Outlooks

1) Electric dipole moment (EDM) search



Parity and Time-reversal violating beyond SM physics
(appears in CP-violating coupling constant g).

Higher sensitivity via Schiff nuclear moments in heavy nuclei

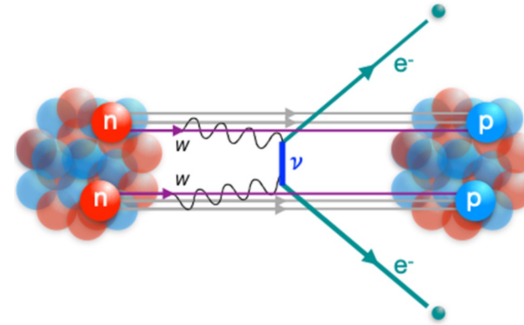
$$S = \langle \Psi \hat{S} \Psi \rangle \propto \bar{g} Z A^{2/3} \langle \beta_2 \beta_3^2 \rangle / \Delta E$$

Octupole deformation enable EDM search

J. Jia, *Rep. Prog. Phys.* 88, 092301 (2025)

Heavy-ion collisions: $R_{v_3^2 \delta p_T} = a - b \langle \beta_2 \beta_3^2 \rangle$

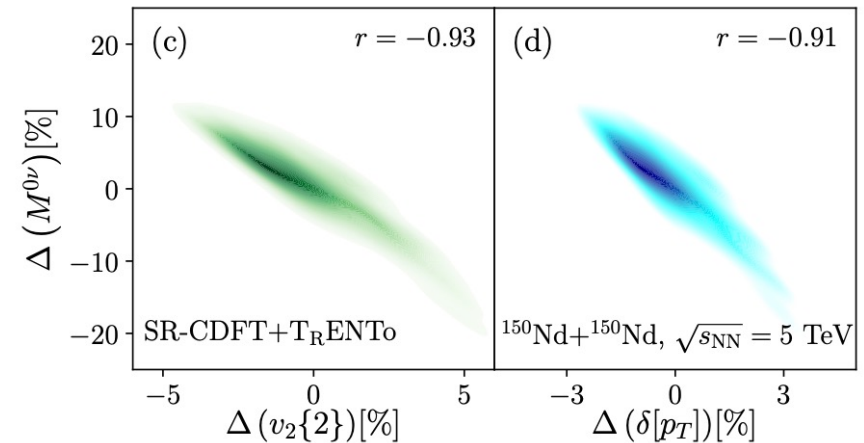
2) Neutrinoless double beta decay



Isotope	$T_{1/2}^{0\nu} (\times 10^{25} \text{ y})$	$\langle m_{\beta\beta} \rangle (\text{eV})$	Experiment
^{48}Ca	$> 5.8 \times 10^{-3}$	$< 3.5 - 22$	ELEGANT-IV
^{76}Ge	> 8.0	$< 0.12 - 0.26$	GERDA
	> 1.9	$< 0.24 - 0.52$	MAJORANA DEMONSTRATOR
^{82}Se	$> 3.6 \times 10^{-2}$	$< 0.89 - 2.43$	NEMO-3
^{96}Zr	$> 9.2 \times 10^{-4}$	$< 7.2 - 19.5$	NEMO-3
^{100}Mo	$> 1.1 \times 10^{-1}$	$< 0.33 - 0.62$	NEMO-3
^{116}Cd	$> 1.0 \times 10^{-2}$	$< 1.4 - 2.5$	NEMO-3
^{128}Te	$> 1.1 \times 10^{-2}$	—	—
^{130}Te	> 1.5	$< 0.11 - 0.52$	CUORE
^{136}Xe	> 10.7	$< 0.061 - 0.165$	KamLAND-Zen
	> 1.8	$< 0.15 - 0.40$	EXO-200
^{150}Nd	$> 2.0 \times 10^{-3}$	$< 1.6 - 5.3$	NEMO-3

Nuclear matrix element

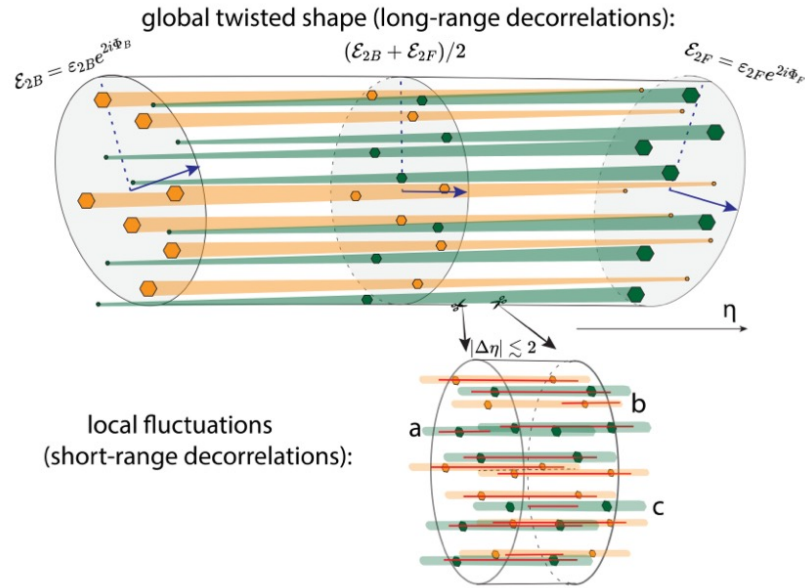
$$T_{1/2}^{0\nu} = \left(G |\mathcal{M}|^2 \langle m_{\beta\beta} \rangle^2 \right)^{-1} \simeq 10^{27-28} \left(\frac{0.01 \text{eV}}{\langle m_{\beta\beta} \rangle} \right)^2 \text{ y}$$



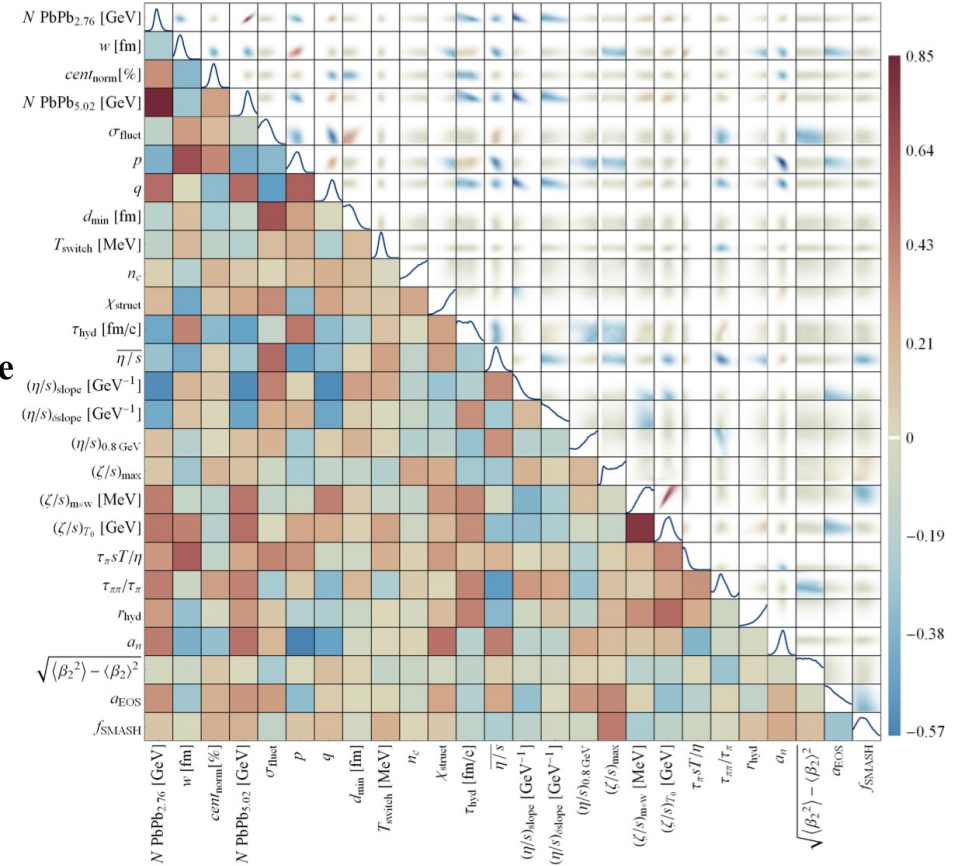
Y. Li, X. Zhang, G. Giacalone, J. Yao, *PRL* 135, 022301 (2025)

IV. Conclusions and Outlooks

3) 3D structure and precise constraints on QGP initial conditions



Bayesian Interference



Isolate the decorrelation map of deformation-induced component:

v_n decorrelations:

C. Zhang, S. Huang, J. Jia, *2405.08749*

J. Jia, S. Huang, C. Zhang, S. Bhatta, *2408.15006*

p_T decorrelations:

L. Liu, J. Chen, X.-G. Huang, J. Jia, C. Shen, C. Zhang, *2511.11094*

J. Zhu, X.-Y. Wu, G.-Y. Qin, *2602.04148*

S. Jahan, Roch, C. Shen, *PRC 113, 024919 (2026)*

G. Giacalone, G. Nijs, W. Schee, *PRL 131, 202302 (2023)*

S. Jahan, Roch, C. Shen, *PRC 113, 024919 (2026)*

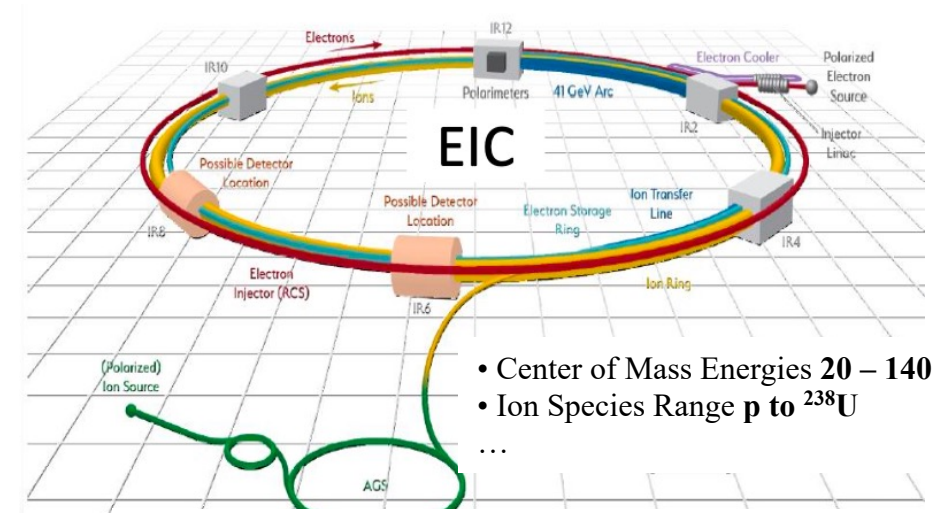
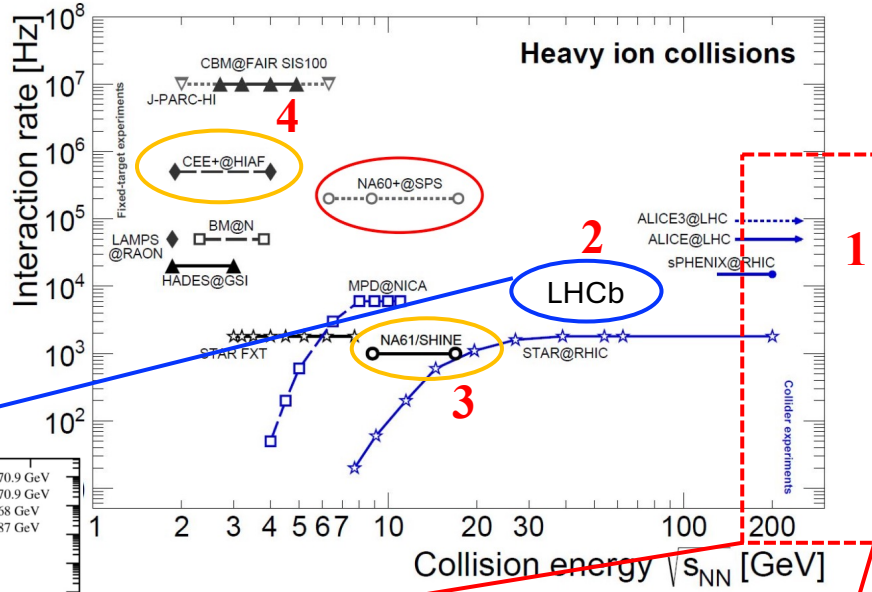
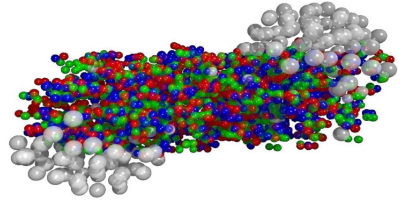
J.E. Bernhard, J.S. Moreland, S.A. Bass, *Nature Physics 15, 1113 (2019)*

D. Everett et al. (JETSCAPE), *PRL 126, 242301 (2021)*

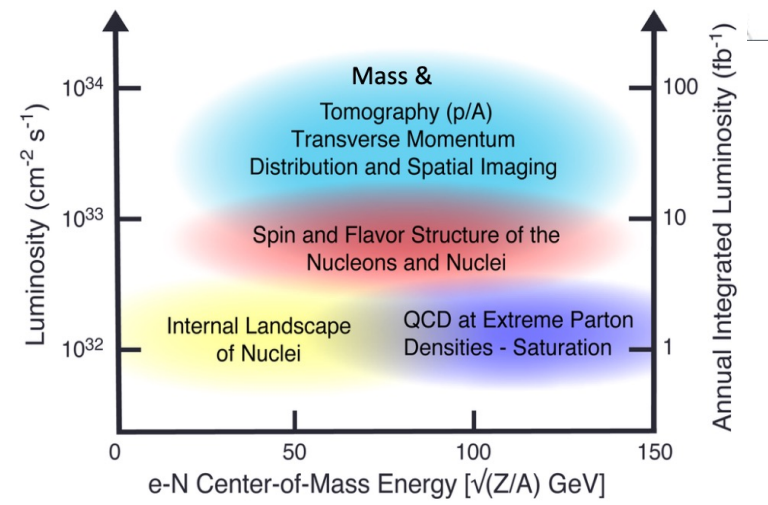
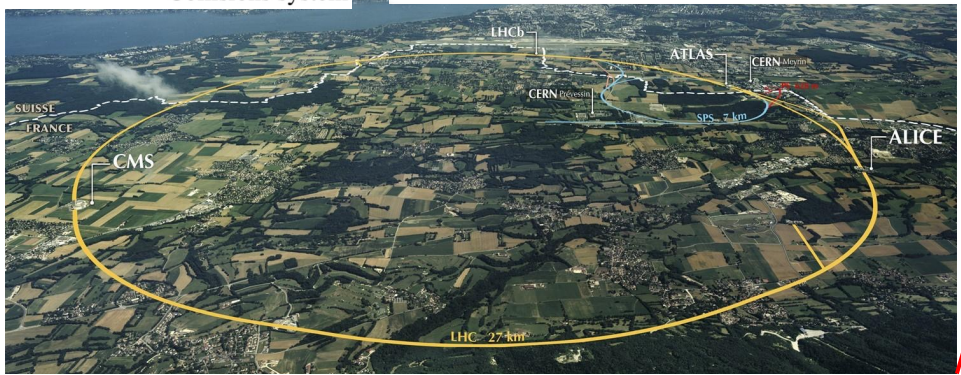
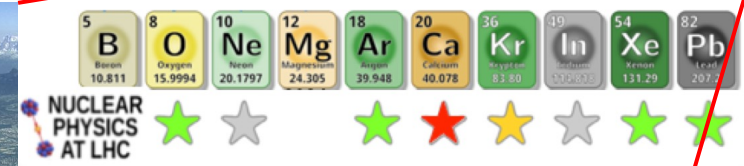
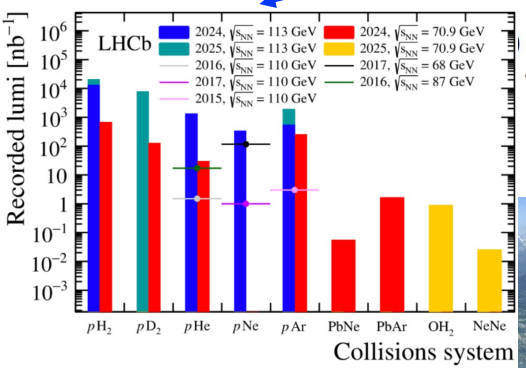
...

IV. Conclusions and Outlooks

4) Energy evolution of nuclear structure, System scan, and the forward-rapidity DIS

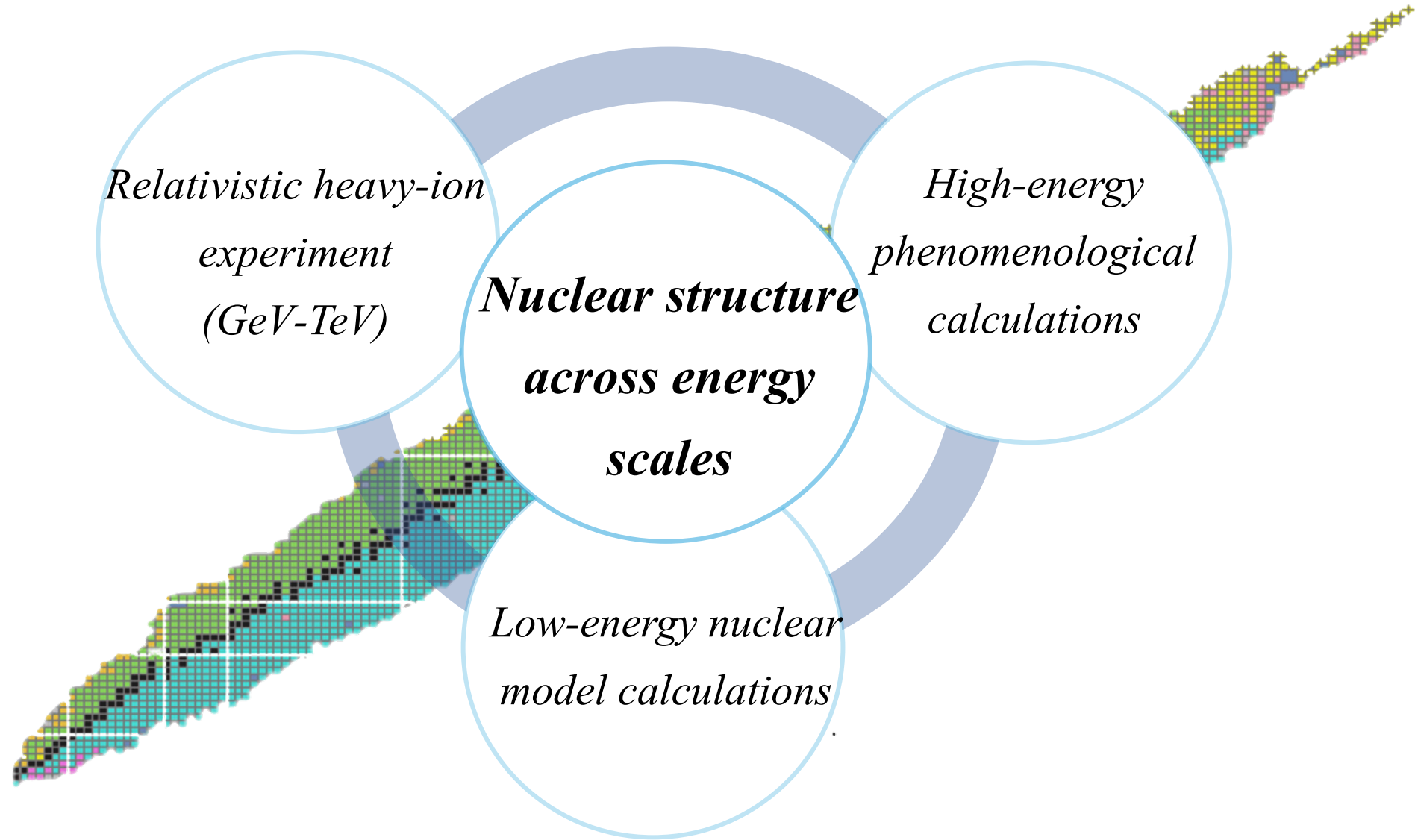


- Center of Mass Energies 20 – 140 GeV
- Ion Species Range p to ²³⁸U
- ...



H. Mantysaari, B. Schenke, C. Shen, W. Zhao, *PRL* 131, 062301 (2023)
 H. Li, L. Liu, J. Chen, Y.-G. Ma, C. Zhang, *CPL* (In press)

IV. Conclusions and Outlooks



Collaboration with nuclear structure and intermediate energy

Acknowledgement



Thank you